Lawrence Berkeley National Laboratory
LBL Publications

Title
Modeling nuclear waste disposal in crystalline rocks at the Forsmark and Olkiluoto repository sites — Evaluation of potential thermal—mechanical damage to repository excavations

Permalink
https://escholarship.org/uc/item/39m6v83p

Authors
Rutqvist, J
Tsang, C-F

Publication Date
2024-10-01

DOI
10.1016/j.tust.2024.105924

Copyright Information
This work is made available under the terms of a Creative Commons Attribution License, available at https://creativecommons.org/licenses/by/4.0/

Peer reviewed

eScholarship.org Powered by the California Digital Library
University of California

Tunnelling and Underground Space Technology 152 (2024) 105924

Contents lists available at ScienceDirect

Tunnelling and Underground Space Technology incorporating Trenchless Technology Research

journal homepage: www.elsevier.com/locate/tust

Modeling nuclear waste disposal in crystalline rocks at the Forsmark and Olkiluoto repository sites – Evaluation of potential thermal–mechanical damage to repository excavations

J. Rutqvist [a,*], C.-F. Tsang [a,b]

[a] Energy Geosciences Division, Lawrence Berkeley National Laboratory, Berkeley, CA, USA
[b] Department of Earth Sciences, Uppsala University, Sweden

ARTICLE INFO

Keywords:
Nuclear waste disposal
Coupled processes modeling
Thermal-mechanical
Excavation damage
Saturation
Bentonite

ABSTRACT

We conduct coupled thermo-hydro-mechanical modeling of a KBS-3V repository design in crystalline rocks, using data and conditions from the Forsmark in Olkiluoto repository sites in Sweden and Finland. The study focuses on repository performance related to the impact of thermal and hydraulic evolution on the potential for thermal–mechanical damage to underground repository excavations. For the designs and conditions considered at the Forsmark and Olkiluoto repository sites, the simulations show a peak temperature well under the adopted performance target of a 100°C maximum temperature, whereas there is still a high potential for thermal–mechanical damage to the KBS-3V waste deposition holes. The thermal–mechanical damage is much more likely if rock permeability is so low that it delays saturation and swelling of bentonite-clay-based backfill beyond the time for the thermal–mechanical peak, which occurs 50 to 100 years after nuclear waste deposition. We also found that sidewalls of the KBS-3V emplacement tunnels are vulnerable to tensile fracturing due to the combined effect of thermal stressing and backfill swelling. The study highlights a strong interaction between bentonite-based backfill and host rock through capillary suction along with induced rock desaturation. A careful design and selection of the bentonite-clay-based backfill materials for KBS-3V tunnels and deposition holes can facilitate a timely saturation and backfill swelling that in turn can minimize thermal–mechanical damage.

1. Introduction

Crystalline rocks, such a granite and gneiss are considered a potential host rock for disposal of high-level radioactive nuclear waste in a number of countries, including Sweden, Finland, Korea, Canada and China (NWTRB, 2022; Faybishenko et al., 2016). Most progress has been achieved in Sweden and Finland with actual selected disposal sites and licenses to go ahead with the repository construction (NWTRB, 2022; Zou and Cvetkovic, 2023). The disposal design in both Sweden and Finland are based on the KBS-3V concept (Fig. 1b), involving emplacement of the waste in a mined repository at about 500 m depth (SKBF/KBS, 1983; SKB, 2006; 2022a; Posiva, 2012a; Hedin and Olsson, 2016). In the KBS-3V concept, the waste is encapsulated in copper canisters that are placed in vertical deposition holes in the floor of waste emplacement tunnels. The copper canisters are embedded in a bentonite-clay-based material that should work as a buffer to protect the canisters against rock movements. The emplacement tunnels are also backfilled with a material that can provide stability of the tunnel walls. Based on such a design, the KBS-3V repository concept consists of multiple barriers that together should function to isolate the nuclear waste from the human accessible environment. These barriers include the encapsulating waste canisters as well as the tight bentonite buffer and host rock that should delay and dilute the transport of radionuclides, if released from a waste canister (Ahn and Apted, 2010; Hedin and Olsson, 2016; Zou and Cvetkovic, 2023).

In Sweden and Finland, the Forsmark and Olkiluoto sites located in Precambrian crystalline rocks of the Fennoscandian Shield are undergoing comprehensive site investigations for waste disposal (Fig. 1a). The Swedish Nuclear Fuel and Waste Management Company (SKB) investigated two candidate sites, Laxemar and Forsmark, until 2009, when Forsmark on the Swedish east coast was selected as the preferred site (Hedin and Olsson, 2016). In 2022, after review by the Swedish Radiation Safety Authority (SSM), and by the Swedish Land and Environment Court, the Swedish Government approved SKB's final repository system

* Corresponding author.
E-mail address: jrutqvist@lbl.gov (J. Rutqvist).

https://doi.org/10.1016/j.tust.2024.105924
Received 29 April 2024; Received in revised form 20 June 2024; Accepted 24 June 2024
Available online 4 July 2024
0886-7798/© 2024 The Author(s). Published by Elsevier Ltd. This is an open access article under the CC BY license (http://creativecommons.org/licenses/by/4.0/).

the license to start the construction at Forsmark (NWTRB, 2022). Site investigations by the Finish Radioactive Waste Management Organization (Posiva) focuses on the Olkiluoto site on the Finish west coast (Siren, 2017; Sedeer, 2022). As part of the site investigations at Olkiluoto, an underground research laboratory (ONKALO) was constructed from 2004 to 2014 (Vira, 2006; Posiva, 2003; Siren, 2017). In 2015, a construction license for a deep geological repository at Olkiluoto was granted by the Finish Government, and in 2021 the construction of the repository tunnels began. Meanwhile, in December 2021, Posiva submitted an operation license application that is currently under review by the Finish Radiation and Nuclear Safety Authority (STUK) with the final assessment on repository operation expected in 2024.

This paper presents numerical modeling of coupled thermo-hydro-mechanical (THM) evolution of a KBS-3V repository in crystalline rocks, using data and conditions from the Forsmark and Olkiluoto repository sites. The objective of the study is to investigate repository performance issues around thermal and hydraulic evolutions, and their impact on the potential for thermal–mechanical damage to KBS-3V underground excavations. Damage to excavations is relevant to repository performance as it can create permeable flow paths that could impact radionuclide transport properties. In this study, two different models, the Forsmark model and the Olkiluoto model are developed considering the range of conditions and properties derived from the site descriptive models of the two sites. The host rocks at Forsmark and Olkiluoto are characterized as sparsely fractured with spacing between water bearing fractures large as 250 m at Forsmark and 50 m at Olkiluoto (Geier et al., 2012). Nuclear waste emplacement in such sparsely fractured crystalline rock is considered as one of the most favorable options, because their high strength and low heat sensitivity, permeability, and dissolution properties, thereby providing a high degree of structural and environmental stability (Zou and Cvetkovic, 2023). On the other hand, disposal in sparsely fractured crystalline rocks maybe be vulnerable to thermal–mechanical damage to underground excavations as well as fracture shear activation due to high and anisotropic in situ stress that is further amplified as a results of high thermal stressing of stiff host rock (Millard et al., 2005; Kwon et al., 2006; Min and Stephansson, 2013; Lee et al., 2020; Seo et al., 2024). Moreover, sparsely fractured rock with its low permeability may lead to a delayed saturation and swelling of the backfill that can impact the function of the backfill to stabilize excavation walls (Nguyen et al., 2009). These are all issues being addresses in this modeling study considering conditions and data from the Forsmark and Olkiluoto sites.

Previous research have shown the importance of coupled THM processes and thermal–mechanical damage for the repository performance and design in hard fractured rocks, such as granite and gneiss. This includes research in the U.S. nuclear waste disposal program that in the 1980s investigated different host rocks, around the Nevada Test Site, in Nevada, including Yucca Mountain (Tyler et al., 1980; Tsang, 1987). The site investigations at Yucca Mountain provided an outstanding data set, one that has significantly advanced our knowledge of coupled THM processes in partially saturated fractured rocks (Rutqvist and Tsang, 2012). Investigations in the Canadian nuclear waste disposal program on rock mechanics and coupled THM processes resulted in groundbreaking research on stress-induced damage to excavations at the Underground Research Laboratory in Manitoba, Canada (Martin et al., 1997; Martino and Chandler, 2004). This include the discovery of the brittle spalling phenomenon on excavation walls that would occur at a compressive stress level much lower than the uniaxial compressive strength on core samples (Martin, 1997). Similar observations on spalling failure were later made at the Äspö Hard Rock Laboratory in Sweden (Andersson et al., 2009a; 2009b). The potential for brittle spalling failure along deposition holes and tunnels is an important part the performance assessment that is being evaluated in the Swedish nuclear waste program (Martin, 2005; Hökmark et al., 2010). For example, Hökmark et al. (2010) found that for the Forsmark site, spalling failure could likely occur due to high thermal stresses. As a result, it is currently assumed in the safety assessment that a spalling zone of high permeability will occur along the deposition holes at Forsmark (Hökmark et al., 2010; SKB, 2022a). Site investigations at ONKALO for the Olkiluoto site, have indicated quite different behavior in which excavation walls may be damaged by yield along host rock foliations rather than brittle spalling (Valli et al., 2023). These differences in the potential and type of thermal–mechanical damage at Forsmark and Olkiluoto are discussed further in the THM analysis and damage assessment presented in this article. In addition to such site-specific observations and analyses, generic modeling studies have been performed to estimate long-term THM repository responses in hard fractured rocks, including work within the international DECOVALEX projects (Birkholzer et al., 2019). In those generic modeling studies, the important interaction between the buffer and the host rock has been investigated related to potential rock damage for both vertical and horizontal emplacement designs (e.g. Millard et al., 2005; Nguyen et al., 2009; Rutqvist et al., 2009b). Related to repository designs, recent work in the Korean nuclear waste disposal program investigates multi-layer disposal concepts for optimizing the storage efficiency in crystalline rock considering limits on the

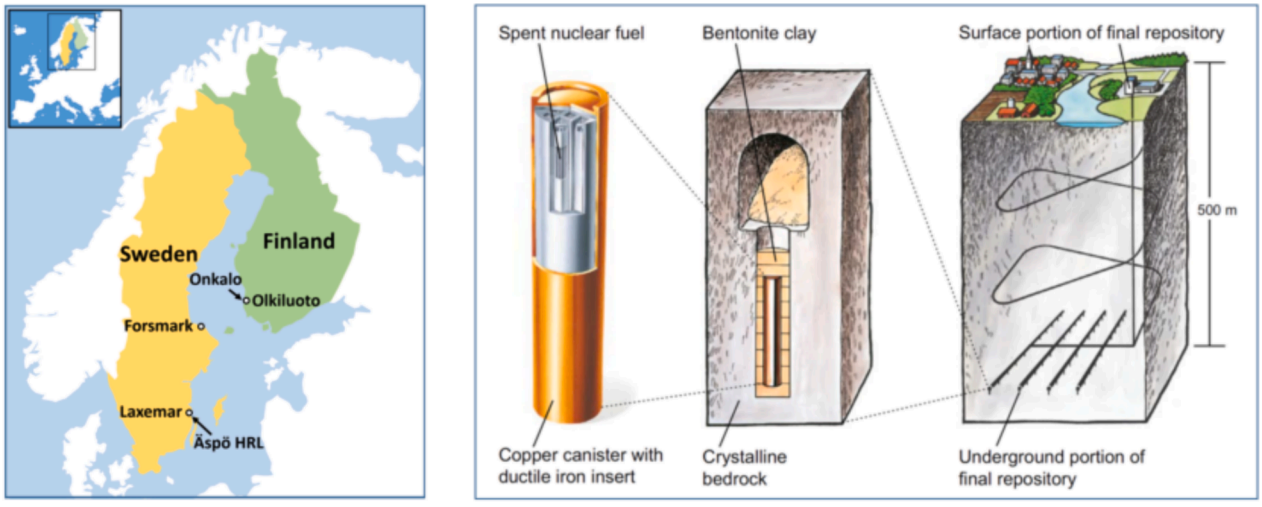

Fig. 1. (a) Locations of the Forsmark and Olkiluoto repository sites in Sweden and Finland considered in this study with other facilities indicated, and (b) schematic of a KBS-3V repository (modified from SKB 2022a).

maximum temperature and rock mechanical stability (Lee et al., 2020; Kim et al., 2024). Overall, these site-specific and generic repository studies show that coupled THM modeling is an important tool for evaluating the long-term performance and designs of repositories in any type of host rock.

The coupled THM analysis of the Forsmark and Olkiluoto sites presented in this article is not part of the regular performance assessment of these sites by SKB and Posiva, but provides an alternative independent analysis performed using an independent numerical model. We begin the description of this analysis in Section 2 by describing the coupled THM model, including the numerical simulator and model set up, as well as derivation of input parameters from the Forsmark and Olkiluoto site descriptions. Some significant differences in conditions and properties between the Forsmark and Olkiluoto sites considered in this study include (1) differences in rock stresses and bedrock strength, (2) differences in rock permeability and permeable fracture spacing, (3) difference in thermal properties, and (4) differences in repository design regarding canister and tunnel spacing (Geier et al., 2012). In Section 3, we describe our approach and model to evaluate the potential for thermal–mechanical damage to underground excavations considering the difference in rock strength between Forsmark and Olkiluoto. Section 4 presents coupled THM modeling results for two simulation cases of high and low rock permeability to study the impact of the buffer and backfill saturation process on the potential thermal–mechanical damage. This is followed in Section 5 by a sensitivity study to investigate the time to saturate the backfill necessary for swelling and support of excavation walls. In Section 6, our results are summarized and discussed in terms of KBS-3V repository performance related to (1) thermal evolution and peak temperature, (2) hydrological evolution and buffer/backfill saturation time, and (3) mechanical evolution, including potential rock damage around underground excavations. We compare these results to independent analyses administered by SKB and Posiva related to the Forsmark and Olkiluoto repository sites (e.g. Hökmark et al., 2009; 2010; Åkesson et al., 2010; Ikonen and Raiko, 2012; Valli et al., 2021; SKB 2022b). We end with concluding remarks regarding our results related to the Forsmark and Olkiluoto models, along with general findings and recommendations on prediction of coupled THM evolution and potential thermal–mechanical damage associated with KBS-3V nuclear waste disposal in crystalline rocks.

2. Coupled THM model

This section presents the coupled THM model, including numerical simulator, model geometry, material properties and simulation steps, along with initial and boundary conditions. The models developed here are denoted the Forsmark model and the Olkiluoto model, that are based on data from the two repository sites.

2.1. Coupled THM numerical simulator

The numerical modeling is conducted with the coupled THM numerical simulator ROCMAS (Noorishad and Tsang, 1996; Rutqvist et al., 2001a; 2005; 2009a). In ROCMAS, the formulation of coupled thermo-hydroelasticity in terms of Biot's theory of consolidation (Biot, 1941) is extended to partially saturated porous media through Philip and de Vries' (1957) theory for heat and moisture flow in soil (Noorishad and Tsang, 1996; Rutqvist et al., 2001a). In this theory, three phases (solid, liquid, and gas) are present, but the gas pressure is constant and equal to atmospheric pressure in a static gas phase, equivalent to Richards' approach in unsaturated groundwater flow modeling (Richards, 1931). Vapor transport occurs through molecular diffusion driven by a gradient in vapor concentration (density) in the static gas phase, while advection of vapor with bulk gas flow is neglected. The vapor density in the medium is governed by Kelvin's relation in the form of the Ostwald–Freundlich equation (Freundlich, 1909) assuming thermodynamic equilibrium for pore liquid in contact with its vapor, and phase transitions occur as evaporation–condensation processes. The mechanical behavior of the porous media consists of the gas, liquid and solid-matter responses to local pressure and the overall material (skeleton) response to effective stresses (Rutqvist et al., 2001a).

With this approach and these assumptions, three balance equations—water mass balance, energy conservation and linear momentum balance—and a number of constitutive relations are required for a full description of the THM state. In ROCMAS, the final governing equations are discretized using a standard Galerkin finite element solution approach to obtain a set of coupled matrix equations that are integrated in time using a finite difference scheme and solved fully coupled (Noorishad and Tsang, 1996; Rutqvist et al., 2001a).

Relevant for the analysis of the potential for thermal–mechanical damage around excavation are models for the evolution of effective stress in the host rock and swelling stress in the bentonite-based backfill materials. In this study, the effective stress for the host rock is calculated according to a Bishop's type of effective stress expressed as

$$\boldsymbol{\sigma}' = \boldsymbol{\sigma} - \mathbf{I} S_l P_l \tag{1}$$

where $\boldsymbol{\sigma}'$ and $\boldsymbol{\sigma}$ are respectively effective and total stress tensors (compression positive), $\mathbf{I}$ is the identity tensor, and S_l and P_l are saturation and pressure of the liquid phase. Furthermore, the mechanical constitutive behavior in ROCMAS is expressed as (Rutqvist et al., 2001a)

$$\mathrm{d}\boldsymbol{\sigma} = \mathbf{D} : (\mathrm{d}\boldsymbol{\varepsilon} - \mathrm{d}\boldsymbol{\varepsilon}_{\mathbf{T}} - \mathrm{d}\boldsymbol{\varepsilon}_{\mathbf{sw}}) = \mathbf{D} : (\mathrm{d}\boldsymbol{\varepsilon} - \mathbf{I}\beta_T dT - \mathbf{I}\beta_{sw}\mathrm{d}S_l) \tag{2}$$

where $\mathbf{D}$ is the tangential stiffness matrix, and $\boldsymbol{\varepsilon}$, $\boldsymbol{\varepsilon}_T$, $\boldsymbol{\varepsilon}_{\mathrm{sw}}$ are tensors of total, thermal, and swelling strains, respectively. In Equation (2), β_T and β_{sw} are respectively the coefficient of linear thermal expansion and the coefficient of linear swelling. That is, swelling strain and swelling stress is analogous to that of thermal strain and thermal stress, and is a linear function of the change in liquid saturation. Such a linear swelling model is a rational approach for modeling the swelling stress evolution in a clay-basted buffer or backfill using a calibrated maximum confined swelling stress at full saturation (Rutqvist et al., 2001a; 2001b; Rutqvist et al., 2011). This swelling model has shown reasonable agreement with stress evolution observed in laboratory tests on bentonite samples (Chijimatsu et al., 2009) and field experiments involving a bentonite buffer (Chijimatsu et al., 2005).

The ROCMAS simulator has been extensively applied for modeling coupled THM processes associated with nuclear waste disposal and tested within the international DECOVALEX project, including verification against hypothetical benchmark tests, code-to-code verification, and validation against laboratory and large-scale field experiments (Rutqvist et al., 2001b; 2005; 2008; 2009b; 2011; Alonso et al., 2005; Nguyen et al., 2001; 2009). A comparison of ROCMAS simulation results with those of full multiphase fluid flow simulations have shown that the Philip and de Vries' (1957) theory as implemented in ROCMAS is adequate for modeling coupled THM processes in the near field of a nuclear waste repository (Wang et al., 2011; Rutqvist et al., 2011).

2.2. Model geometry

The periodicity of a KBS-3V repository design with fixed spacing between deposition holes and between tunnels, allows for reducing the model domain to a one-quarter symmetric three-dimensional model (Fig. 2). The quarter symmetric geometry represents a condition that neighboring deposition holes are simultaneously excavated and heated and this may best represent the conditions at the center of a repository. We include relevant components associated with the Engineered Barrier System (EBS) of the KBS-3V repository, including heat releasing waste, waste canister, bentonite buffer, tunnel backfill, and surrounding near field rock. Models developed for each of the Forsmark and Olkiluoto sites have site-specific depth and model dimensions. The model dimensions are defined according to the respective suggested repository layouts that have been evaluated by thermal management analyses for

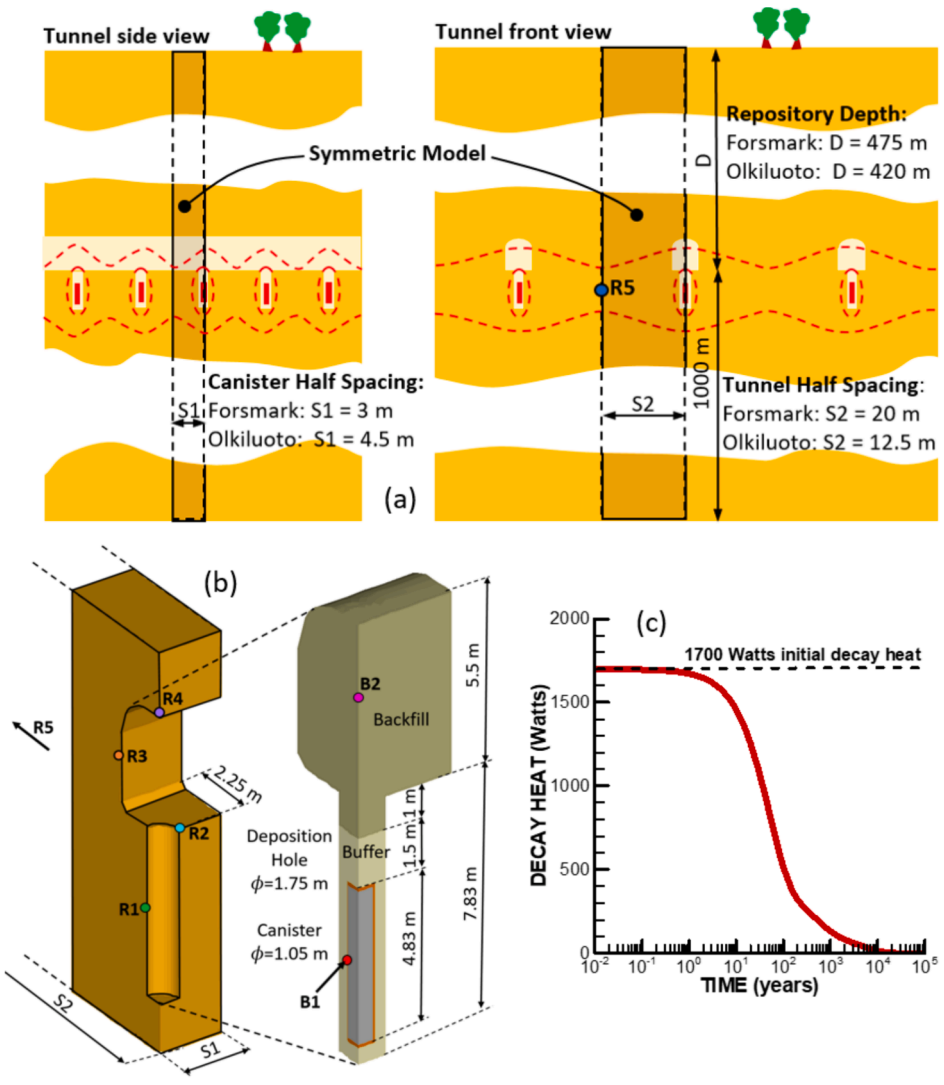

Fig. 2. Three-dimensional model geometry of a KBS-3V deposition hole in the middle of a repository. (a) Tunnel side and front views illustrating the symmetric temperature evolution with model dimensions for the Forsmark and Olkiluoto models, (b) near-field model geometry with monitoring points in the buffer, backfill and host rock, and (c) decay heat function for one canister starting at an initial power of 1700 W (heat decay function originates from Hökmark et al., 2009).

the Forsmark and Olkiluoto repositories (Hökmark et al., 2009; Ikonen and Raiko, 2012; SKB, 2022b; Ikonen et al., 2018; Valli et al., 2021). At Forsmark, for a tunnel spacing of 40 m, the minimum canister spacing is set to 6 m (SKB, 2022b), while at Olkiluoto for a tunnel spacing of 25 m, the spacing between canisters is longer (Ikonen et al., 2018; Valli et al., 2021) and here taken as 9 m. Such differences in the tunnel spacing and deposition hole spacing along with differences in the initial stress field, affect the thermal–mechanical stress evolution and the potential for damage of the underground excavations.

2.3. Buffer and backfill properties

The material properties for the bentonite buffer and backfill were defined considering comprehensive experimental investigations reported over three decades by SKB and Posiva (Börgesson and Hernelind, 1999; Börgesson et al., 2006; 2009; Johanesson and Nilsson, 2006; Autio et al., 2012; Dueck and Nilsson, 2010; Åkesson et al., 2010; SKB, 2022d). There is a close collaboration between SKB and Posiva regarding the buffer and backfill and the material selection may change in the future. The material properties of the buffer and backfill in our base-case simulation correspond to in-situ compacted MX-80 bentonite for the buffer and a backfill material consisting of a mixture of bentonite and crushed rock with a weight ratio of 30/70. Most properties for this type of buffer and backfill were extracted from Börgesson and Hernelind (1999) and Börgesson et al. (2006) involving model calibration and validation against laboratory experiments (Rutqvist and Tsang, 2008; Chijimatsu et al., 2009). Such backfill and similar buffer material were also used by SKB at the Äspö Hard Rock Laboratory Prototype Repository (Börgesson et al., 2002; Cleall et al., 2006).

From around 2010, both SKB's and Posiva's KBS-3V designs have involved placement of pre-compacted bentonite blocks in both deposition holes and tunnels along with granular bentonite in construction gaps (Åkesson et al., 2010; Autio et al., 2012; SKB 2022d). Most recently, Posiva changed backfill selection to emplacement of granulated bentonite (Posiva, 2021). Thus, the buffer and backfill properties applied in the base-case of this study may not be the latest or final selection by SKB and Posiva, but is a realistic set of properties representative for a KBS-3V repository in crystalline rocks. In addition to the 30/70 backfill applied in the base-case, a number of alternative backfill options are considered in a sensitivity study focusing on hydraulic behavior and buffer saturation. These include properties for Friedland clay extracted from Börgesson et al. (2006), as well as granular MX-80 bentonite and pre-compacted blocks of MX-80 with homogenized properties taken from Åkesson et al. (2010) and SKB (2022d).

Base-case material properties, i.e. for the in-situ compacted MX-80 buffer and 30/70 backfill are presented in Table 1, while properties for liquid phase (water) flow are presented in Table 2 for all relevant materials, including the buffer, the four backfill options, and the host rock. For the water retention, the original van-Genuchten model (van-Genuchten, 1980) is used along with the following modified version due to Gens et al. (2009) for a better representation of the retention properties at low liquid saturation

$$S_l = \left[1 + \left(\frac{s}{P_0}\right)^{\frac{1}{1-\lambda_0}}\right]^{-\lambda_0} \times \left(1 - \frac{s}{P_d}\right)^{\lambda_d} \quad (3)$$

where s is capillary suction, and P_0, λ_0, P_d, and λ_d are model parameters. In this equation, the first part is the original van-Genuchten model, defined by the capillary scaling parameter P_0 and the shape parameter λ_0.

Fig. 3 shows the water retention and relative permeability curves for the buffer and different backfill options along with the curves assumed for the host rock. The figure illustrates very large variations in capillary suction and liquid phase permeability between buffer, rock and different backfill options. Included in Fig. 3 and listed in Table 2 are also the initial conditions, i.e. the initial saturation, capillary suction and liquid phase permeability. For example, for the buffer (green curves in Fig. 3), the initial liquid saturation at emplacement of the buffer is 0.61, which corresponds to an initial capillary suction of 33 MPa and a liquid phase permeability of about 9×10^{-22} m^2.

The calibration of the maximum swelling stress for the bentonite buffer and backfill requires an estimated average bulk modulus, K, and the moisture swelling coefficient β_{sw}. These two parameters are estimated from experimental data for MX-80, presented in Börgesson and Hernelind (1999). First, a moisture swelling coefficient of $\beta_{sw} \approx 0.4$ is determined by fitting to data from unconfined drying shrinkage test. Moreover, experimental data in Börgesson and Hernelind (1999) indicate a swelling stress of 6 to 8 MPa when a sample is wetted to full saturation from an initial saturation of 61 %. With a target swelling stress of 8 MPa, a representative average bulk modulus for the linear swelling model would be 17 MPa. Same approach was used to derive parameters for the backfill to achieve a target swelling stress of about 3 MPa upon full saturation.

2.4. Rock properties

Table 3 lists rock properties for the Forsmark and Olkiluoto models. As mentioned in the introduction, there is a difference in the occurrence of water conducting fractures and host rock permeability at Forsmark and Olkiluoto (Geier et al., 2012). The apparent spacing between water conducting fractures detected by borehole flow logging is about 50 m at Olkiluoto, while as large as 250 m at Forsmark (Geier et al., 2012). Block-scale permeability has been estimated to range from $1x10^{-19}$ m^2 to $1x10^{-17}$ m^2, whereas unfractured matrix permeability could be as low as $1x10^{-21}$ m^2 (Geier et al., 2012; Vaittinen et al., 2020; Åkesson et al., 2010; Vilks, 2007). Acknowledging this variability, we treated rock permeability as a parameter that locally around each deposition hole could vary many orders of magnitude. We considered extreme cases of high and low rock permeability that would result in respectively relatively fast and slow saturation of the EBS. For the case in which saturation would be relatively fast, the host rock permeability was set to 1.0×10^{-16} m^2. A permeability 1.0×10^{-16} m^2 is close the mean permeability of the previous candidate site in Sweden, Laxemar, in fractured crystalline rocks, while the permeability at the selected Forsmark and Olkiluoto sites is generally much lower as they are sparsely fractured with fewer water bearing fractures. For the case in which saturation would be relatively slow, the host rock permeability was set to 1.0×10^{-20} m^2. A permeability 1.0×10^{-20} m^2 may correspond to unfractured matrix permeability. The water retention curve of the host rock is taken from Finsterle and Pruess (1995), who back-calculated the retention curve using inverse modeling of two-phase flow processes at a tunnel ventilation experiment in fractured granite.

Among other host rock properties listed in Table 3, we can observe a marked lower rock thermal conductivity at Olkiluoto compared to Forsmark. Moreover, the Young's modulus is lower at Olkiluoto, while the thermal expansion coefficient is higher. Such difference in properties have an impact on temperature and thermal–mechanical responses as well as on the potential for thermal–mechanical damage to the underground excavations.

Table 1
Base-case material parameters for the MX-80 bentonite buffer and 30/70 backfill.

Parameter	MX-80 Bentonite Buffer	30/70 Backfill
Permeability, k	6.5×10^{-21}	0.5×10^{-17}
Relative permeability, k_r [-]	$k_r = S^3$	$k_r = S^{10}$
Bulk Modulus, K [MPa]	17	17
Porosity, ϕ [-]	0.435	0.363
Bulk Modulus, K [MPa]	17	17
Poisson ratio, ν [-]	0.3	0.3
Biot's constant, α [-]	0.0 ($P_l < 0.0$) 1.0 ($P_l \geq 0.0$)	0.0 ($P_l < 0.0$) 1.0 ($P_l \geq 0.0$)
Swelling coefficient, β_{sw} [-]	0.4	0.14
Thermal expansion, β_T [1/°C]	1.0×10^{-5}	1.0×10^{-5}
Dry specific heat, C_{vs} [J/kg·°C]	800	800
Thermal conductivity, [W/m·°C]	$\lambda = 0.3$ ($S_l \leq 0.25$) $\lambda = 0.3+(S_l-025) \times 0.8$ ($0.25 < S_l < 0.8$) $\lambda = 1.3$ ($S_l \geq 0.8$)	$\lambda = 0.3$ ($S_l \leq 0.25$) $\lambda = 0.3+(S_l-025) \times 0.8$ ($0.25 < S_l < 0.8$) $\lambda = 1.3$ ($S_l \geq 0.8$)

2.5. Simulation steps with boundary and initial conditions

The simulations consider relevant repository construction and operation stages of (1) pre-excavation equilibrium, (2) excavation (3), waste, buffer and backfill emplacement, and (4) post closure. The initial conditions defined at the pre-excavation equilibrium stage, including vertical gradients of temperature, fluid pressure, and in situ stress, are extracted from the site descriptive models along with recent updates (SKB, 2008; SKB, 2022c; Figuiredo et al., 2022; Mattila et al., 2022; Posiva, 2012b; 2021). A pre-excavation simulation is conducted to achieve an accurate initial equilibrium condition with applied boundary conditions. In this modeling, all lateral model boundaries are closed for flow of heat or fluid and with the condition of zero normal displacement. Such lateral boundaries are justified by the symmetric conditions for the quarter symmetric model (Fig. 2). The top and bottom boundaries are held at constant pressure and temperature. Mechanically, the top boundary representing the ground surface is free to move vertically and while a zero normal displacement condition is imposed at the bottom boundary.

The excavation sequence (excavation and operational period) is simulated for 10 years, assuming tunnels open at atmospheric pressure. For both the Forsmark and Olkiluoto models, the tunnels were assumed to be oriented parallel to the maximum stress according to the repository designs for respective site. The initial temperature, fluid pressure, vertical and horizontal principal stresses at the repository depth are listed in Table 4.

The stress field for the Forsmark model is adopted from the recent Forsmark site data report SKB, 2022c, in turn based on the Forsmark rock mechanics site descriptive model (Glamheden et al., 2007). At 475 m depths, the vertical stress is 14 MPa, maximum compressive horizontal stress parallel to the tunnel axis is 41 MPa and minimum compressive horizontal stress normal to the tunnel axis stress is 23 MPa. For the Olkiluoto model, we adopted the regional stress field defined as the most likely stress in Figuiredo et al. (2022). This is a vertical stress of

Table 2
Saturated and unsaturated liquid phase fluid flow properties including water retention and relative permeability along with initial conditions.

Parameter	Buffer	Backfill Options				Rock	
	MX-80	30/70	Friedland	Granular	Blocks	High Perm	Low Perm
Permeability, k [m^2]	6.5×10^{-21}	5.0×10^{-18}	7.0×10^{-19}	5.2×10^{-19}	4.8×10^{-21}	1.0×10^{-16}	1.0×10^{-20}
Rel. permeability k_{rl} [-]	$k_{rl} = S_l^4$	$k_{rl} = S_l^{10}$	$k_{rl} = S_l^3$	$k_{rl} = S_l^3$	$k_{rl} = S_l^3$	vG-M*	vG-M*
Equation (3), P_0 [MPa]	18	0.109	1.1	0.162	11.6	5.5	5.5
Equation (3), λ_0 [-]	0.333	0.194	0.248	0.187	0.231	0.667	0.667
Equation (3), P_d [MPa]	400	500	500	NA	NA	NA	NA
Equation (3), λ_d [-]	1.0	0.09	0.09	0.0**	0.0**	NA	NA
Initial saturation [-]	0.606	0.592	0.296	0.267	0.639	1.0	1.0
Initial Suction	33.0	0.9	36.4	46.0	46.0	0	0
Initial liquid phase permeability [m^2]	8.77×10^{-22}	2.64×10^{-20}	1.82×10^{-20}	1.33×10^{-20}	1.25×10^{-21}	1.0×10^{-16}	1.0×10^{-20}
Initial porosity [-]	0.435	0.363	0.410	0.630	0.425	0.01	0.01

* Relative permeability defined by van Genuchten-Mualem (vG-M) model (Mualem, 1976; van Genuchten, 1980).
** With $\lambda_d = 0.0$, the original van Genuchten water retention model is retained (van Genuchten, 1980).

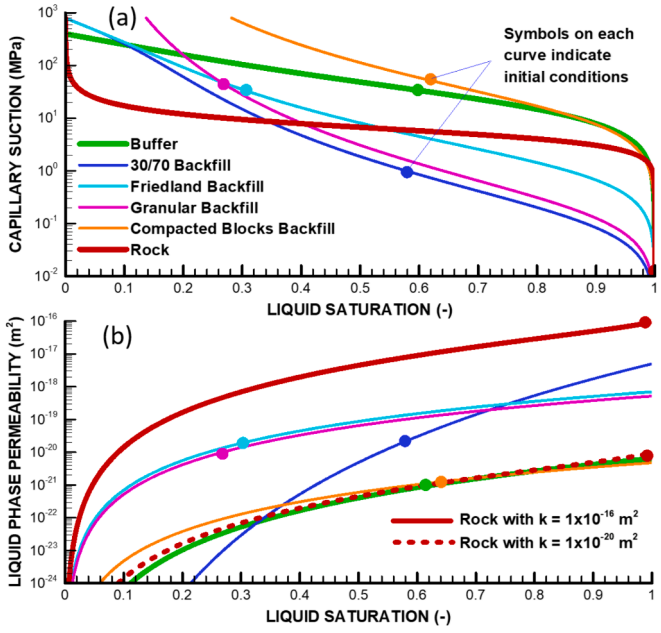

Fig. 3. (a) Water retention and (b) liquid phase permeability curves for the buffer, host rock, and different backfill options. The symbols on each curve marks initial conditions of saturation, capillary suction and liquid phase permeability.

Table 3
Base-case rock properties for the Forsmark and Olkiluoto models.

Parameter	Forsmark Model	Olkiluoto Model
Density, ρ_s [kg/m^3]	2701	2764
Porosity, ϕ [-]	0.01	0.01
Young's Modulus, E [GPa]	68 GPa	55 GPa
Poisson's Ratio, ν [-]	0.22	0.26
Biot's coefficient, α [-]	1.0	1.0
Specific heat, C_v [J/kg·°C]	800	800
Thermal conductivity, K_m [W/m·°C]	3.46	2.57
Thermal expansion, β [1/°C]	7.7×10^{-6}	9.24×10^{-6}
Hydraulic permeability, k {m^2]	1.0×10^{-16} (high) 1.0×10^{-20} (low)	1.0×10^{-16} (high) 1.0×10^{-20} (low)

11 MPa consistent with the weight of the overburden, while the maximum compressive horizontal stress parallel to the tunnel axis is 20 MPa and the minimum compressive horizontal stress normal to the tunnel axis is 15 MPa. This is somewhat different from the analyses made by Valli et al., (2021) in which the all three stresses are slightly higher based on stress estimates at ONKALA. Overall, the stress field at

Table 4
Initial host rock conditions for the Forsmark and Olkiluoto models before excavation.

Parameter	Forsmark Model	Olkiluoto Model
Depth [m]	475	420
Pressure [MPa]	4.75	4.20
Temperature [°C]	11.7	11.0
Vertical stress	14	11
Maximum horizontal stress [MPa]	41	20
Minimum horizontal stress [MPa]	23	15

repository depth applied in the Forsmark model is much higher and much more anisotropic compared to the stress field applied in the Olkiluoto model.

After 10 years, the waste canister, bentonite buffer, and backfill are installed instantaneously and the post-closure simulation begins with a heat source applied within the waste canister. The adopted power of heat release from each canister is shown in Fig. 2c and originates from Hökmark et al. (2009). This function has previously been applied in various thermal design analyses and THM modeling related to both the Swedish and Finish nuclear waste disposal programs (e.g. Hökmark et al., 2010; Toprak et al., 2012; Suikkanen et al., 2016; Valli et al., 2021), The Swedish repository system is designed for an average power of 1700 W at disposal, that can be achieved for both BWR and PWR assemblies by considering different burn-up and interim storage times (e.g. 35 or 40 years). The heat decay function with 1700 W initial power has also been applied for the Finish repository system for disposed BWR fuel (Ikonen and Raiko, 2012; Toprak et al., 2012). The repository post-closure is simulated for 100,000 years until the temperature and fluid pressure and stress have been restored to ambient conditions.

3. Rock damage potential

In this study, we analyze the potential for rock damage rather than a full analysis of the rock failure processes. The approach is to calculate the evolution of the stress field caused by thermally-driven coupled THM processes and then apply a failure criterion to investigate the potential for damage. Since this study focuses on potential damage on the excavation walls, an in situ strength is considered that could be much lower than conventional uniaxial compressive strength determined on core samples. For example, a simple failure criterion under compressive stress expressed by Martin (2005) stipulates that brittle failure, so-called spalling failure, of an unsupported excavation wall would be initiated when the maximum principal compressive stress exceeds about 50% of the short-term uniaxial compressive strength determined on core samples. The 50% reduction originally observed in crystalline rock at the Underground Research Laboratory in Manitoba, Canada, may be a result of the difference in stress loading paths (Martin, 1997). Similarly, in situ

spalling experiments conducted at the Äspö Hard Rock Laboratory in Sweden indicated an in situ spalling yield strength of about 125 MPa (Andersson et al., 2009a; 2009b), which was about 59% of laboratory uniaxial compressive strength. These experiments also indicated that a small confining pressure of about 0.150 MPa could suppress the spalling (Andersson et al., 2009b). The observed impact of confining pressure indicates that the swelling stress from the buffer and backfill could have an important function to prevent spalling failure of the excavation walls.

A similar in situ experiment conducted at ONKALO, the Posiva Spalling Experiment (POSE), indicated quite different behavior (Valli et al., 2023). Despite several attempts of heating of the rock to induced thermal compressive stress much above the perceived spalling strength, no brittle spalling failure took place. Instead of spalling, the dominant failure mode at POSE was shear along pronounced foliations surfaces and lithological contacts (Valli et al., 2023). Because of the dominant foliation shear, and the very heterogeneous and foliated nature of the rock at ONKALO and the Olkiluoto site, failure is not expected to be continuous along deposition holes or tunnels. Back analysis from the POSE along with laboratory experiments indicate that such failure along foliations would occur when principal stresses are optimally oriented relative to the foliation plane (Mattila et al., 2022; Valli et al., 2023). Moreover, static loading tests of Olkiluoto samples indicate that the measured crack damage stress can be regarded as a suitable estimate of the long-term strength over which a tunnel remains open (Mattila et al., 2022; Valli et al., 2023).

To consider aforementioned findings from pillar-scale experiments at both Äspö and ONKALO, we will use a more general term of damage rather than spalling. The potential for damage is estimated using a Mohr-Coulomb failure criterion that can account for the impact of confining effective stress, σ'_3, on the rock compressive strength, σ'_{1c}, according to

$$\sigma'_{1c} = C_0 + q\sigma'_3 \tag{4}$$

where C_0 is the uniaxial compressive strength and q is the slope, which both can be calculated from the cohesion and coefficient of friction (Jaeger et al., 2007). Moreover, the evolution of the maximum compressive principal effective stress, σ'_1, and compressive strength, σ'_{1c}, are used to calculate a safety factor as (σ'_{1c}/σ'_1). This is interpreted such that if the calculated maximum compressive principal effective stress is higher than the estimated in-situ compressive strength (i.e. if $\sigma'_1 > \sigma'_{1c}$ and $\sigma'_{1c}/\sigma'_1 < 1$) there is a high potential for damage to the excavation walls.

Fig. 4 presents Mohr-Coulomb envelops and parameters derived from site descriptive and rock mechanics models for the Forsmark and Olkiluoto sites (SKB, 2008; SKB, 2022c; Figuiredo et al., 2022; Mattila et al., 2022; Posiva, 2012b; Valli et al., 2021). The Mohr-Coulomb parameters considered for the Forsmark model is an estimate of rock mass strength from the rock mechanics site descriptive model (Glamheden et al., 2007). The uniaxial compressive strength ($C_0 = 127$ MPa) is close to the observed spalling strength at the Äspö pillar-scale experiment, while the assumed slope ($q = 6.26$) leads to significant impact of the minimum compressive stress. For the Olkiluoto model, the basic Mohr-Coulomb envelope is based on a crack damage stress envelope that has been recommended as suitable estimate of the long-term strength of excavations (Mattila et al., 2022). In addition, Mohr-Coulomb envelops for foliation shear back-calculated by Hakala et al., (2018) from the POSE are considered. However, foliation shear would require that the foliation plane is optimally oriented relative to the maximum compressive stress, which depends on the local foliation orientation. Therefore, the crack damage envelope is our primary damage criterion for the Olkiluoto model, while the potential for foliation shear is also considered. The foliation shear criterion defined for POSE by Hakala et al., (2018) includes the initial strength, followed by cohesion drop and fiction mobilization to a residual strength. Fig. 4 also includes the target swelling pressures for the backfill (3 MPa) and buffer (8 MPa) to indicate the impact that the confining pressure from buffer and backfill swelling could have on the compressive strength of the excavation walls. For

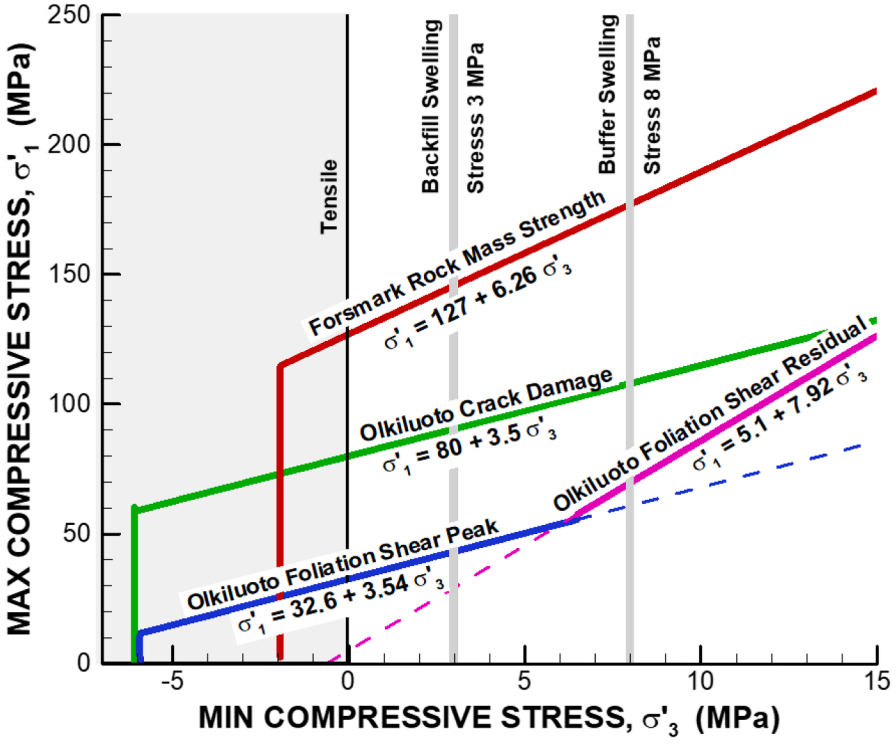

Fig. 4. Mohr-Coulomb failure envelops derived from Forsmark and Olkiluoto site descriptive and rock mechanics models considered in this study for calculating the potential for rock damage to excavations.

example, in the case of Forsmark, the compressive strength, σ'_{1c}, could increase from the uniaxial strength of 127 MPa at zero confining stress to about 180 MPa at 8 MPa confining stress.

4. THM modeling results

In this section, we present the results for the two simulation cases of high and low rock permeability for both the Forsmark and Olkiluoto models. In the case of high rock permeability, the saturation of the buffer and backfill is timely and occurs before the time of the thermal–mechanical peak stress. In the case of low rock permeability, the saturation of the buffer and backfill is slow and does not occur before the time of the thermal–mechanical peak stress. This allow us to study the impact of the buffer and backfill saturation process on the potential for damage to the excavation walls.

4.1. Temperature evolution

Fig. 5 presents the temperature evolution at two points in the EBS (B1 and R1) and one point located away from the emplacement tunnels (R5). The figure illustrates how the peak temperature in the buffer is impacted by the host rock permeability and it also illustrates a difference in the thermal evolution between the Forsmark and Olkiluoto models. In the case of high rock permeability, the maximum temperatures of 72°C (for the Forsmark model), and 76°C (for the Olkiluoto model) are attained at the canister surface (point B1) about 20 years after waste emplacement. In the case of low rock permeability, the maximum temperature increases to 84 °C for the Forsmark model and 94°C for the Olkiluoto model. At the buffer/rock interface (point R1 and green lines in Fig. 5), a maximum temperature of 52°C is attained after 40 years for the Forsmark model, while a maximum temperature of 54 °C is attained for the Olkiluoto model after 60 years. In the host rock, away from the tunnel (point R5 and blue lines in Fig. 5), the peak temperature is 41°C for the Forsmark model and 50°C for the Olkiluoto model. For both site models, the peak temperature in the host rock away from the tunnel occurs after about 100 years with a high-temperature plateau lasting for about 1000 years. Thus, somewhat higher peak temperatures are achieved for the Olkiluoto model, in particular for the host rock temperature, which is a result of the lower rock thermal conductivity of the Olkiluoto host rock. At 30,000 years, when heat power is down to a few percent of its initial value (Fig. 2c) the temperature has declined close its initial value (Fig. 5).

4.2. Evolution of liquid saturation

Fig. 6 presents the evolution of liquid saturation in the buffer, backfill and near-field rock. The evolution of saturation is very similar for the Forsmark and Olkiluoto models, because the hydraulic properties are assumed the same. However, there is a significant difference in the saturation behavior for the high and low rock permeability cases. In the case of high rock permeability, full EBS saturation is reached within 10 years. In the case of low rock permeability, the host rock is desaturated and it takes more than 40,000 years to full saturation of the EBS. The rock desaturates because water is absorbed into the bentonite buffer by a strong capillary suction (much stronger inherent suction than that of the rock) at a rate that cannot be sustained by fluid flow from the surrounding rock. At the same time, a significant drying occurs near the hot waste canister because of evaporation of liquid water to water vapor and its transport along the thermal gradient towards cooler regions of the buffer. The delayed buffer saturation in the case of a low rock permeability implies that the buffer stays relatively dry with a lower thermal conductivity and this is the reason for the higher peak temperature seen in Fig. 5 for the low rock permeability case. When rock permeability is low, the buffer first saturates by water supply from the initial water content in the overlying backfill. After about 2000 years, the buffer has drawn sufficient water from the backfill to be about 90% saturated (Fig. 6). At the same time, the saturation in the backfill has decreased from an initial 59% to 48%. The buffer becomes fully saturated (100%) once the backfill becomes fully saturated by slow water supply from the surrounding low permeability rock.

4.3. Evolution of liquid pressure

Fig. 7 shows the evolution of liquid pressure, which involves capillary suction for unsaturated conditions and restoration of hydrostatic pressure after full saturation. For the backfill design applied in this case, i.e. the 30/70 backfill at 60% initial saturation, the initial suction is relatively low and much lower than that in the buffer. The suction would tend to equilibrate between the backfill, buffer and near field rock, but this takes time because of low permeability in the buffer and host rock. In the case of low rock permeability, the suction is equilibrated between buffer, backfill and near field rock after about 7000 to 10,000 years, while the backfill saturation is still less than 50% and buffer saturation is 98%. Because of the capillary suction interaction with the relatively dry backfill, the buffer cannot be 100% saturated until the backfill is 100% saturated, which takes more than 40,000 years. This indicates that the time to full saturation in both the backfill and buffer is very much

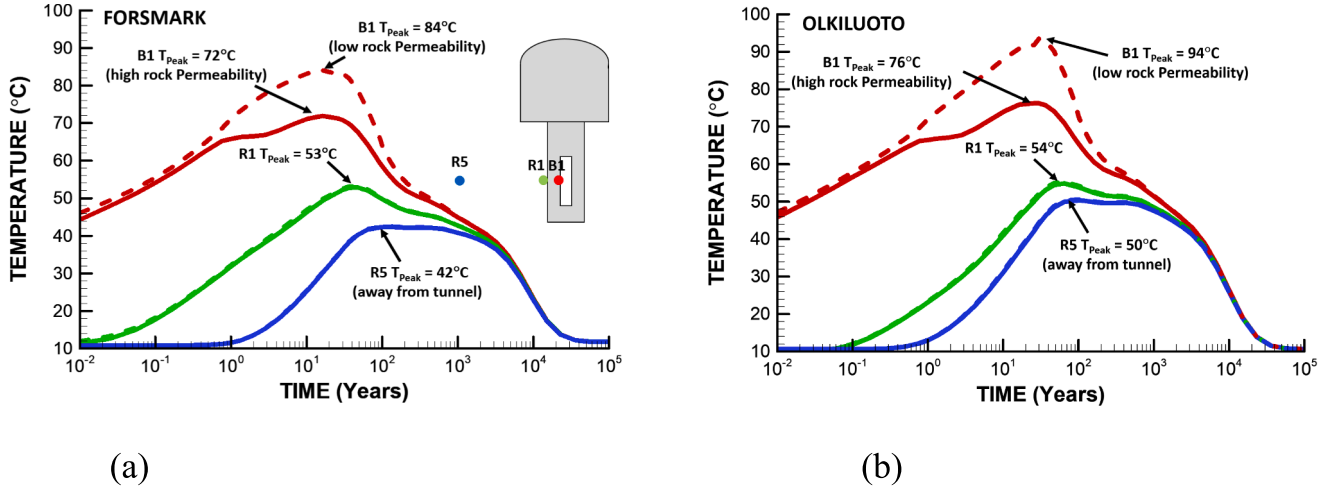

Fig. 5. Temperature evolution with peak temperatures indicated for (a) the Forsmark model and (b) the Olkiluoto model assuming high rock permeability (solid lines) and low rock permeability (dashed lines).

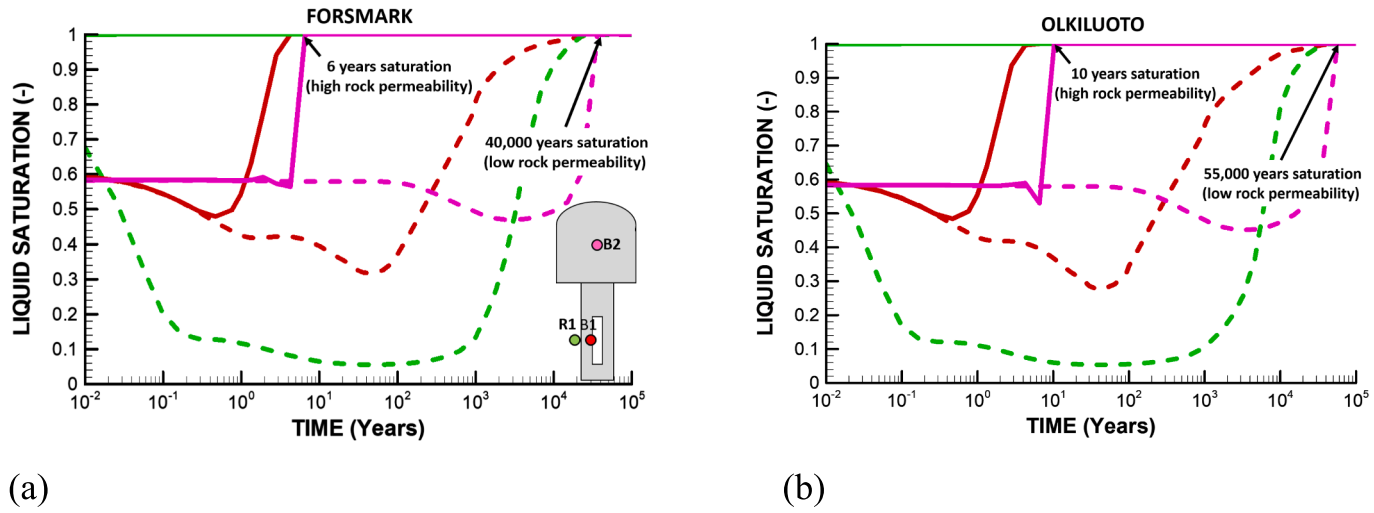

Fig. 6. Saturation evolution with indication of time to full saturation for (a) the Forsmark model and (b) the Olkiluoto model assuming high rock permeability (solid lines) and low rock permeability (dashed lines).

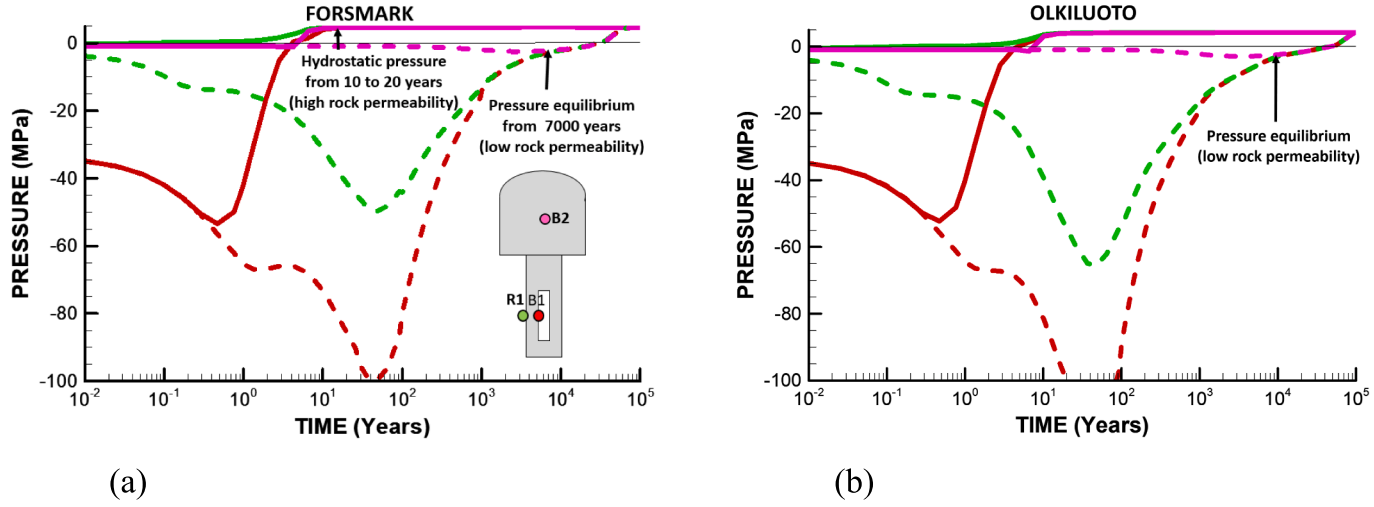

Fig. 7. Pressure evolution with times for restored hydrostatic pressure for (a) the Forsmark model and (b) the Olkiluoto model assuming high rock permeability (solid lines) and low rock permeability (dashed lines).

dependent on the water filling and suction development within the backfill. Fig. 7 also indicates some differences between the Forsmark and Olkiluoto models as the curves of liquid pressure are somewhat different. In the buffer, near the waste canister, the capillary suction decreases more for the Olkiluoto model because of higher temperature and evaporation. In addition, it takes longer for the capillary suction to go to zero (i.e. to full saturation) in the case of the Olkiluoto model compared to that of the Forsmark model.

4.4. Evolution of stress in the buffer and backfill

Fig. 8 presents the evolution of total stress in the buffer and backfill. The final total stress within the buffer and backfill depends on several components. First, the bentonite and backfill swells because of increased liquid saturation. The confinement of the buffer and backfill within excavations results in a swelling stress of about 8 MPa in the buffer and 3 MPa in the backfill. Full saturation and full swelling occur within 10 years in the case of high rock permeability, whereas it takes over 40,000 years in the case of low rock permeability. After fully saturated, the fluid pressure increases from 0 to 4.80 MPa (for the Forsmark model) and from 0 to 4.25 MPa (for the Olkiluoto model), which is consisted with the hydrostatic fluid pressures at mid-canister depth for respective model. Assuming Biot's $\alpha = 1.0$ for the bentonite and backfill, the pressure increase could give rise to an increase in total stress of about 4.8 and 4.25 MPa, respectively. The total stress developed is then the sum of the swelling stress and the fluid pressure increase, along with a small component of a thermal stress, leading to about 12 to 13 MPa total stress in the buffer and 7 to 8 MPa in the backfill (Fig. 8). The swelling stress of 8 MPa in the buffer and 3 MPa the backfill is an effective stress that provides the mechanical confining effective stress on the excavation walls.

4.5. Evolution of stress in the rock and possible damage

Figs. 9 to 11 show the tangential effective stress evolution in the excavation walls at four key locations around the underground excavations. Included in these figures is also the evolution of compressive strength calculated using parameters for the Mohr-Coulomb envelops shown in Fig. 4. An early peak stress at about 50 years occurs at R1, located at the mid-canister height of the deposition hole (green lines in Fig. 9). This point has a relatively high initial tangential compressive stress because of the initial anisotropic horizontal stress field and this

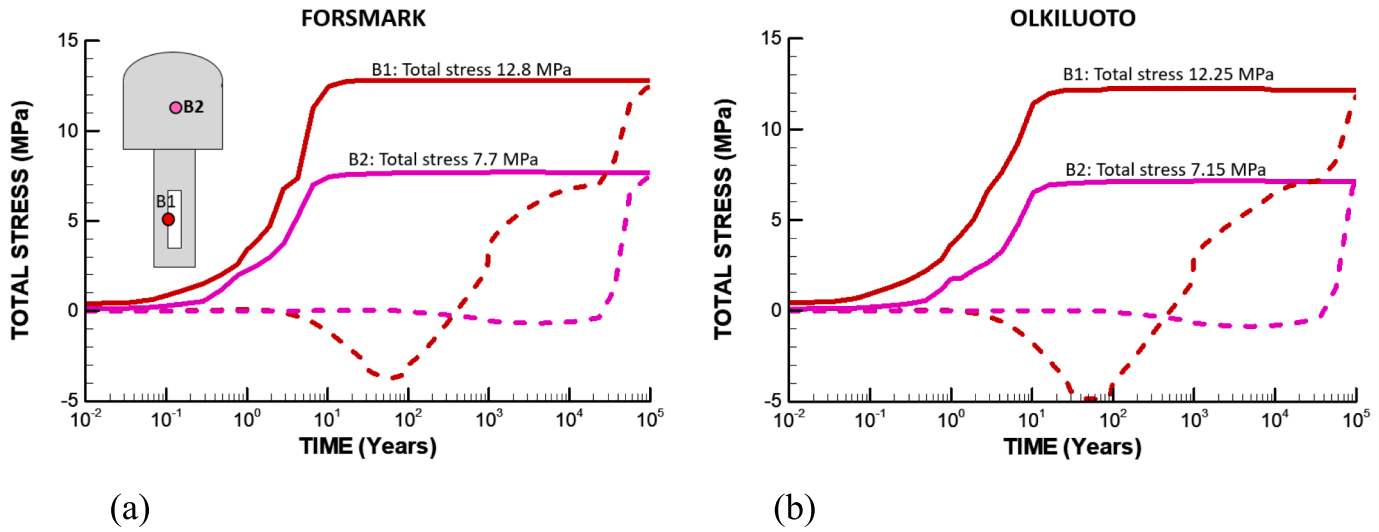

Fig. 8. Stress evolution in the buffer and backfill with time for (a) the Forsmark model and (b) the Olkiluoto model. Results are presented for high rock permeability (solid lines) and low rock permeability (dashed lines).

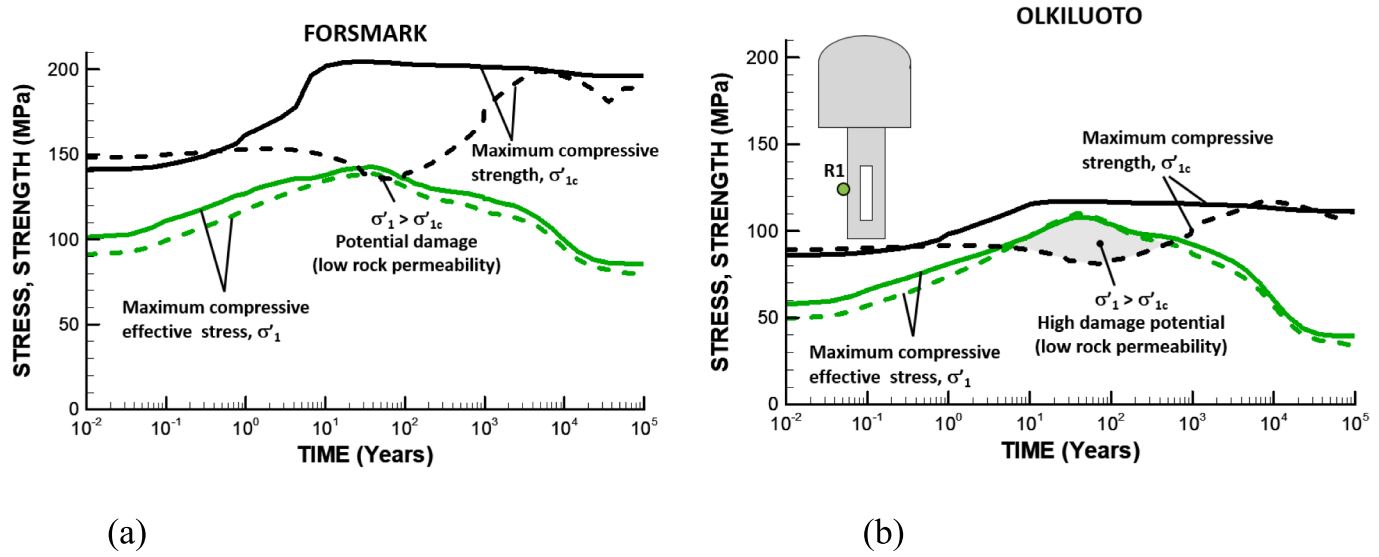

Fig. 9. Stress and strength evolution in point R1 at the deposition hole for (a) the Forsmark model and (b) the Olkiluoto model. Results are presented for high rock permeability (solid lines) and low rock permeability (dashed lines).

tangential compressive stress further amplifies by thermal stressing during rock heating. At about 50 years, the compressive tangential stress in R1 peaks at about 145 MPa for the Forsmark model and at about 109 MPa for the Olkiluoto model. This tangential stress is monitored 1.5 cm from the rock wall of the deposition hole and its location at mid-canister height implies that the local temperature evolution has a significant impact on thermal stress. While the calculated thermal stress increase is about 60 MPa for both the Forsmark and Olkiluoto models, the absolute peak stress is much higher for the Forsmark model, because of the much higher initial maximum compressive horizontal stress.

At R2 and R4, below and above the tunnel, the compressive stresses peak from about 100 years and remain high until more than 1000 years (Figs. 10 and 11). Above the tunnel, in R4, for a monitoring point located 10 cm from the excavation wall, the stress peaks at 75 MPa for the Forsmark model and 70 MPa for Olkiluoto model (orange lines in Fig. 11). Below the tunnel, at point R2, stress peaks as high as 110 to 120 MPa, because of high stress concentration at the intersection with the deposition hole (cyan lines in Fig. 10).

The compressive stress magnitudes at R1, R2 and R4 are important for the potential compressive failure at these locations. Included in the figures are also the evolution of compressive strength based on the Mohr-Coulomb parameters assigned to the Forsmark and Olkiluoto models (black lines in Figs. 9 to 11). The evolution of compressive strength increases along with buffer and backfill saturation and swelling stress. In the case of high rock permeability, the buffer and backfill achieve full saturation and swelling within 10 years and the compressive strength increase to higher values within 10 years (solid black lines in Figs. 9 to 11). As a result, for high rock permeability, the compressive stresses do never exceed the strength, except at point R2 in the case of the Olkiluoto model. In the case of low rock permeability, the results show that compressive tangential stress exceeds the compressive strength at the deposition hole, point R1, for both the Forsmark and Olkiluoto models (dashed green and black lines in Fig. 9). The tangential stress can exceed the strength because the buffer remains dry with no development of confining swelling stress. Below the tunnel, at point R2, no damage is estimated for the Forsmark model, while for the Olkiluoto model there is high potential for damage (Fig. 10). As seen in Fig. 10, the peak compressive stress is similar for the Forsmark and Olkiluoto models

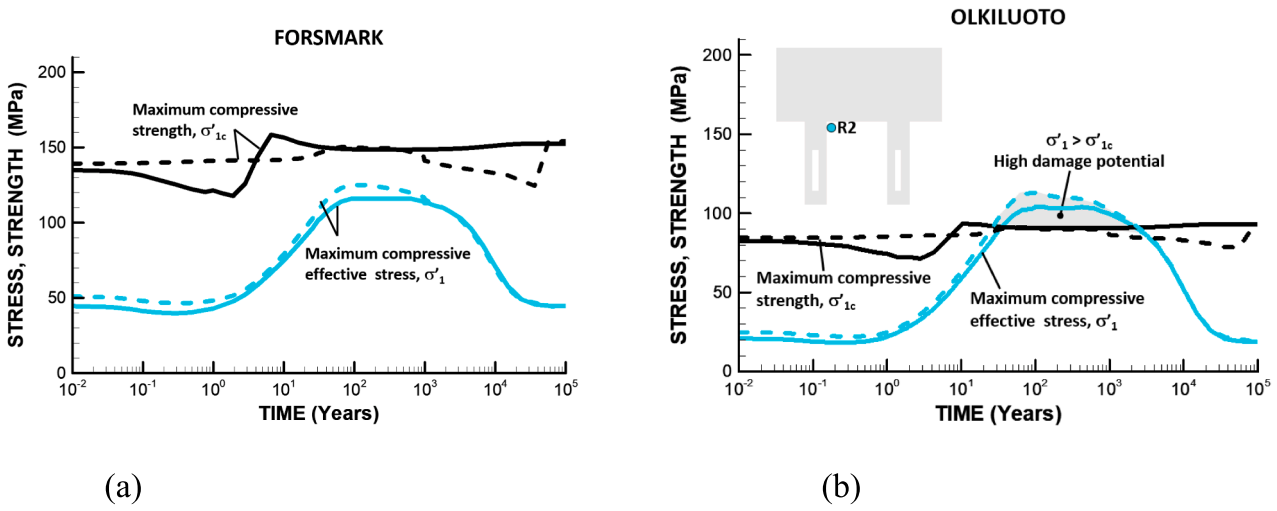

Fig. 10. Stress and strength evolution in point R2 below the tunnel at its intersection with the deposition hole for (a) the Forsmark model and (b) the Olkiluoto model. Results are presented for high rock permeability (solid lines) and low rock permeability (dashed lines).

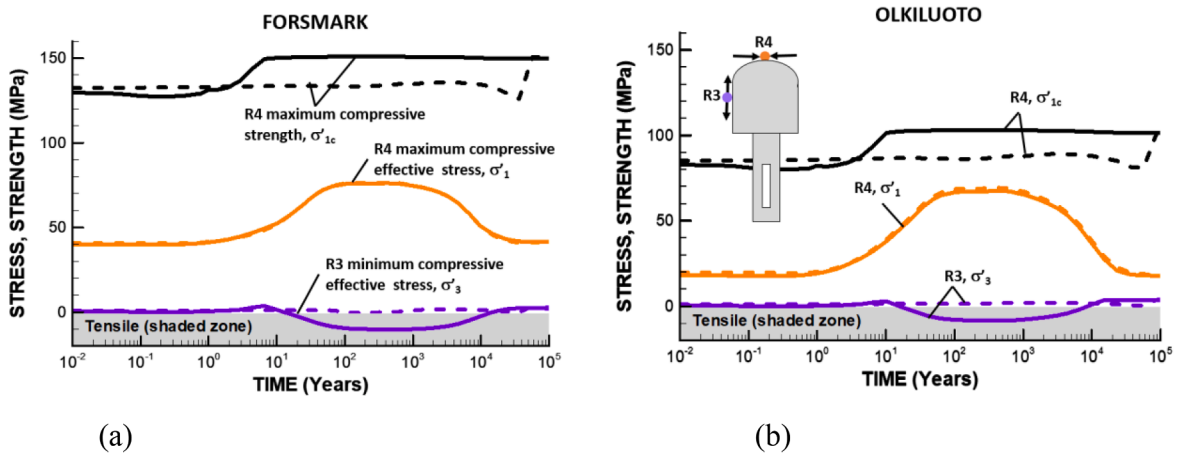

Fig. 11. Stress and strength evolution at the top and side of the emplacement tunnel for (a) the Forsmark model and (b) the Olkiluoto model. Results are presented for high rock permeability (solid lines) and low rock permeability (dashed lines).

(cyan lines in Fig. 10), but the rock strength is much lower for the Olkiluoto model (black lines in Fig. 10). At R4, above the tunnel, no thermal–mechanical damage is anticipated as the strength far exceeds the compressive stresses for both the Forsmark and Olkiluoto models (black lines are much above orange lines in Fig. 11).

For Point R3, on the side of the tunnel, tensile effective stress develops in both the Forsmark and Olkiluoto model simulations for the case of high rock permeability (Fig. 11, solid purple lines). The direction of the tensile stress is vertical and parallel to the tunnel wall, and hence if the rock fails in tension, horizontal fractures could develop along the tunnel axis. This zone of tension develops due to a combination of horizontal repository thermal stress and swelling stress within the backfill, along with the restoration of a hydrostatic fluid pressure. The impact of the repository thermal stress is seen as the tensile stress increases up to about 10 MPa only during the period of high repository temperature and only in the case of high rock permeability when full backfill swelling stress has developed and the fluid pressure has restored to the hydrostatic value of 5 MPa.

Figs. 12 and 13 present contours of minimum and maximum compressive stresses while Fig. 14 shows the resulting contours of the safety factor (σ'_{1c}/σ'_1) at the time of excavation and 100 years after waste emplacement. The figures present results at 100 years for the high rock permeability case when buffer is fully saturated with a fully developed swelling stress and for the low permeability case when the buffer remains dry without any significant swelling stress.

Fig. 12 shows that the highest compressive stress develops around the deposition hole at 100 years, which is due to thermally induced stresses. The maximum compressive stresses are much higher and more concentrated for the Forsmark model, while lower and more uniformly distributed around the deposition hole for the Olkiluoto model. The main reason for this difference in stress concentration is that the in situ stress field is higher and more anisotropic at the Forsmark site. The slight difference in maximum compressive total stress observed in Fig. 12 between low and high permeability cases can be explained by differences in near-field fluid pressure.

Fig. 13 shows the minimum compressive principal stress distributions, which are quite similar for the Forsmark and Olkiluoto models. The minimum compressive principal stress at excavation is impacted by the open tunnel and deposition hole and is therefore close zero around these openings. In the case of high rock permeability and fully developed swelling, the minimum compressive stress increases around the excavations as seen in Fig. 13 by a shift from green to blue contours around the deposition hole. At the same time, a red area contour expands in the tunnel sidewall indicating tensile stress. In the case of low permeability, the stress decreases further near the deposition hole as the buffer remains dry without swelling stress.

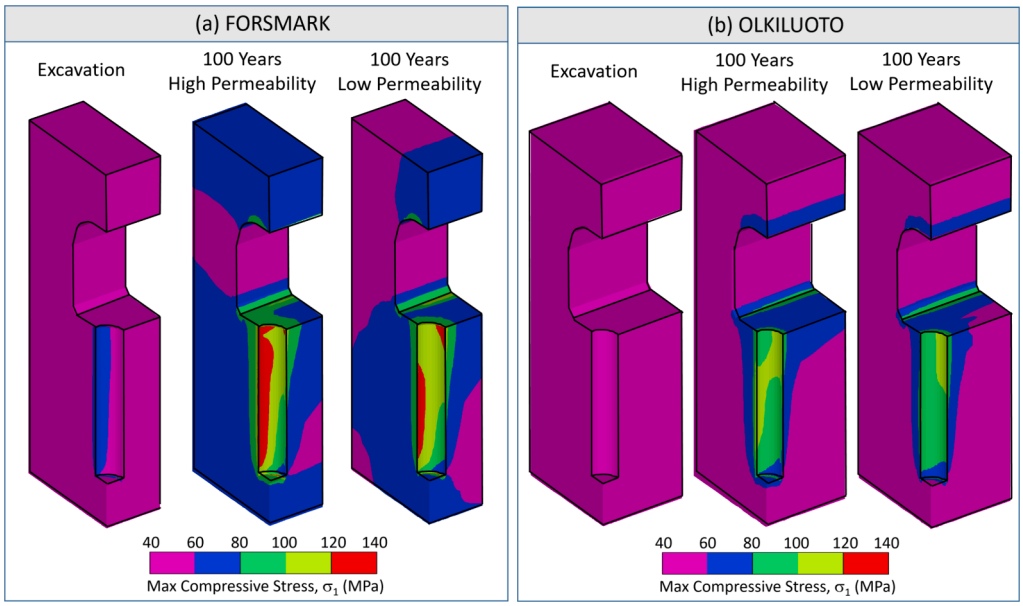

Fig. 12. Maximum compressive principal stress distribution at excavation and at 100 years for high and low permeability cases for (a) the Forsmark model and (b) the Olkiluoto model.

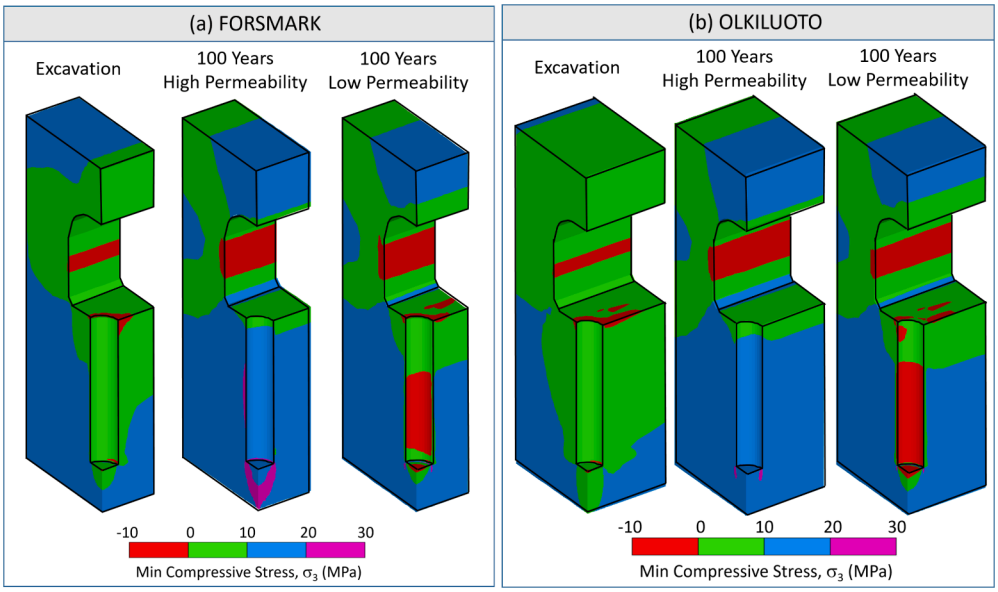

Fig. 13. Minimum compressive principal stress distribution at excavation and at 100 years for high and low permeability cases for (a) the Forsmark model and (b) the Olkiluoto model.

The maximum and minimum compressive stresses shown in Figs. 12 and 13 impact the compressive effective stress and strength and therefore have a significant impact on the contours of the safety factor against damage (σ'_{1c}/σ'_1) in Fig. 14. A safety factor of less than one, i.e. $\sigma'_{1c}/\sigma'_1 < 1.0$, shown as red areas in Fig. 14 indicates areas of high potential for damage. In both the Forsmark and Olkiluoto models there is an increase in red areas of high potential for damage around the deposition hole for the case of low rock permeability. That illustrates the fact that if sufficient saturation and swelling of the buffer does not take place before the thermal–mechanical peak, there will be a much higher potential for thermal–mechanical damage around the deposition holes. On the other hand, for the case of high rock permeability when full saturation is achieved before the thermal–mechanical peak, no widespread damage is indicated around the deposition hole. Only in the Olkiluoto model there is a red area of high damage potential below the tunnel floor at the intersection with the deposition hole.

In Fig. 13b, the white mesh indicates the spatial extent of potential foliation shear ($\sigma'_{1c}/\sigma'_1 < 1.0$) considering the Mohr-Coulomb envelop for foliation shear shown in Fig. 4. The zone of high potential of foliation shear extends approximately 0.4 m up from the crown of the tunnel, about 1 m below the floor of the tunnel, and down to 2.5 m below the floor at the intersection with the deposition hole. The shear stresses in these areas are sufficiently high to induce foliation shear under the condition that the local foliation plane is optimally oriented for shear, i.e. at about 30° relative to the local maximum compressive stress direction.

Finally, the red zone in the sidewall of the emplacement tunnel is the zone of tensile stress and high potential of tensile failure. This is a tangential (vertical) stress that is induced by the combined effect of a thermal-stress relief due to rock heating and a backfill swelling stress of

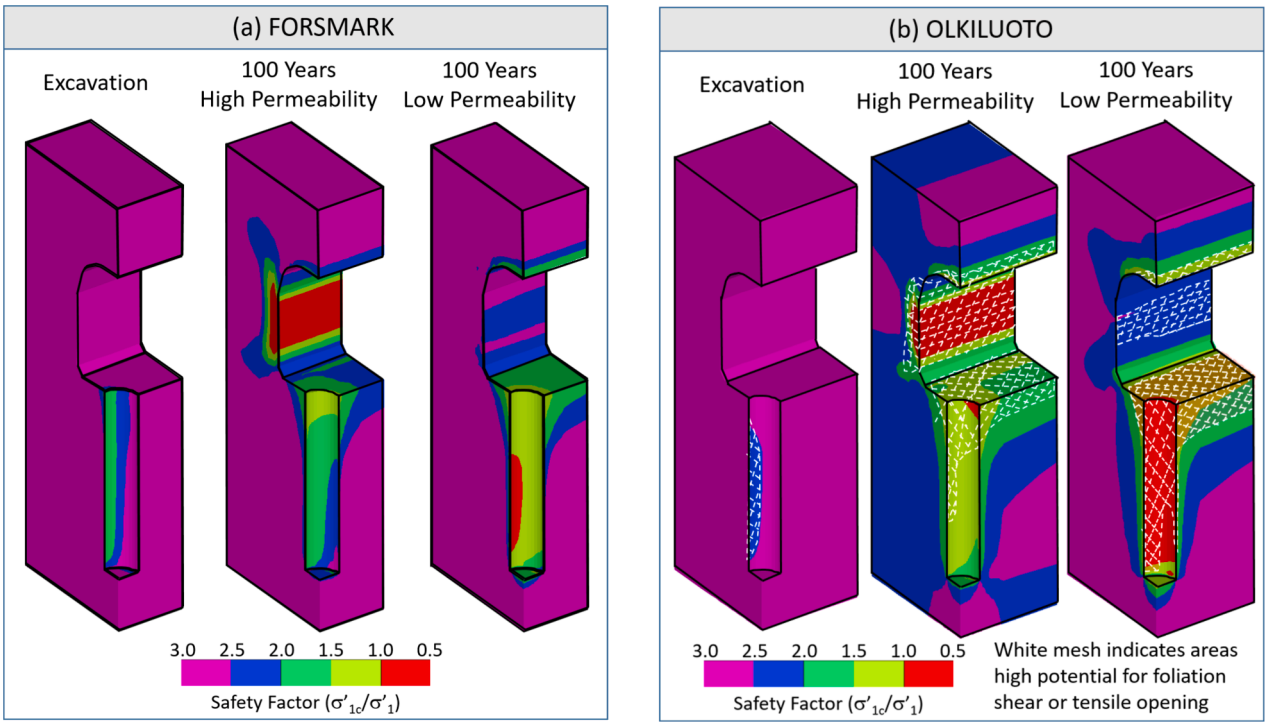

Fig. 14. Safety factor against damage (σ'_{1c}/σ'_1) at excavation and at 100 years for high and low permeability cases for (a) the Forsmark model and (b) the Olkiluoto model. The white mesh in (b) indicates areas of high potential for foliation shear if foliation is optimally oriented for shear.

about 3 MPa within the tunnel, under a hydrostatic fluid pressure of about 5 MPa. Because this tangential (vertical) stress increases up to about 10 MPa tension, it will exceed the tensile strength assumed for the Forsmark and Olkiluoto models according to tension cut-off of the Mohr-Coulomb envelops in Fig. 4. The zone of high potential for tensile failure does not occur in the case of low permeability rock, because the backfill is dry with a lack of swelling stress and local fluid pressure is negative.

5. Sensitivity study of resaturation time

This section presents a sensitivity study on the buffer and backfill saturation time, considering the impact of rock permeability, backfill options, and distance to water feeding boundaries. The sensitivity study is performed using the Forsmark model with the understanding that the results would be similar for the Olkiluoto model. Fig. 15 presents the results in terms of rock permeability versus saturation time for various conditions. Saturation time to either 99% or 90% liquid saturation are considered. Marked in these figures are the approximate time of the thermal–mechanical peak, i.e. 50–100 years from waste emplacement.

Fig. 15a and 15b present the saturation times for different backfill options considering the various retention and relative permeability functions shown in Fig. 3. The results in Fig. 15a shows that 99 % saturation would not be achieved in the buffer before the thermal–mechanical peak, unless rock permeability is $1x10^{-17}$ m^2 or higher. The only exception is for the 30/70 backfill option when a permeability of $1x10^{-18}$ m^2 would be sufficient to achieve 99 % as the buffer draws water from the backfill by capillary suction. Fig. 15b shows that a 90 % saturation can be achieved within the buffer before the thermal–mechanical peak if the rock permeability exceeds $3x10^{-19}$ m^2, while a 90 % backfill saturation would require a permeability of about $1x10^{-17}$ m^2. The 90 % saturation time for a backfill consisting of pre-compacted blocks is quite different from other backfill options (Fig. 15b, green lines). As shown in Fig. 3 the pre-compacted blocks option has a low initial permeability, but at the same time a high initial suction.

Fig. 15c and d show the impact of the distance to a water-feeding boundary for the case of 30/70 backfill. In addition to the base-case of the water feeding from the ground about 400 to 500 m away, two other cases assume water-feeding boundaries at 20 and 100 m distances. These are realistic cases considering that the spacing of water bearing fractures at Forsmark can be 250 m and 50 m at Olkiluoto (Geier et al., 2012). The simulations assume that the pressure is constant at the water-feeding boundaries and therefore can provide unlimited water supply. From Fig. 15c and d it appears that the distance to the water-feeding boundary has most significant impact on the backfill saturation times. For example, reducing the distance from 500 to 100 m, reduces the saturation time by an order of magnitude. The impact of the distance to the water-feeding boundary is less prominent for the buffer saturation time and the results generally show that a rock permeability of $1x10^{-19}$ m^2 would be required to achieve 90 % saturation before the thermal–mechanical peak.

6. Summary and discussion

The modeling results are summarized and discussed in terms of (1) thermal evolution and peak temperature, (2) hydrological evolution and saturation time, and (3) mechanical evolution and thermal–mechanical damage to excavations. The results are discussed in the light of results of other studies in the literature, including studies of the Forsmark and Olkiluoto repository sites.

6.1. *Thermal evolution and peak temperature*

The thermal evolution and peak temperature need to be accurately evaluated as part of the thermal management of any repository (Hökmark et al., 2009; Ikonen and Raiko, 2012; Rutqvist, 2020). The performance target for the KBS-3 repository concept in the Swedish and Finnish nuclear waste repository programs is a maximum temperature of 100°C to assure chemical stability of the buffer (Posiva-SKB, 2017). Our analysis shows that the peak temperature would not exceed 80°C, if buffer saturation is timely, and would not exceed 95°C even if saturation delays beyond the time of the thermal–mechanical peak. The temperature evolutions calculated here are consistent with temperature

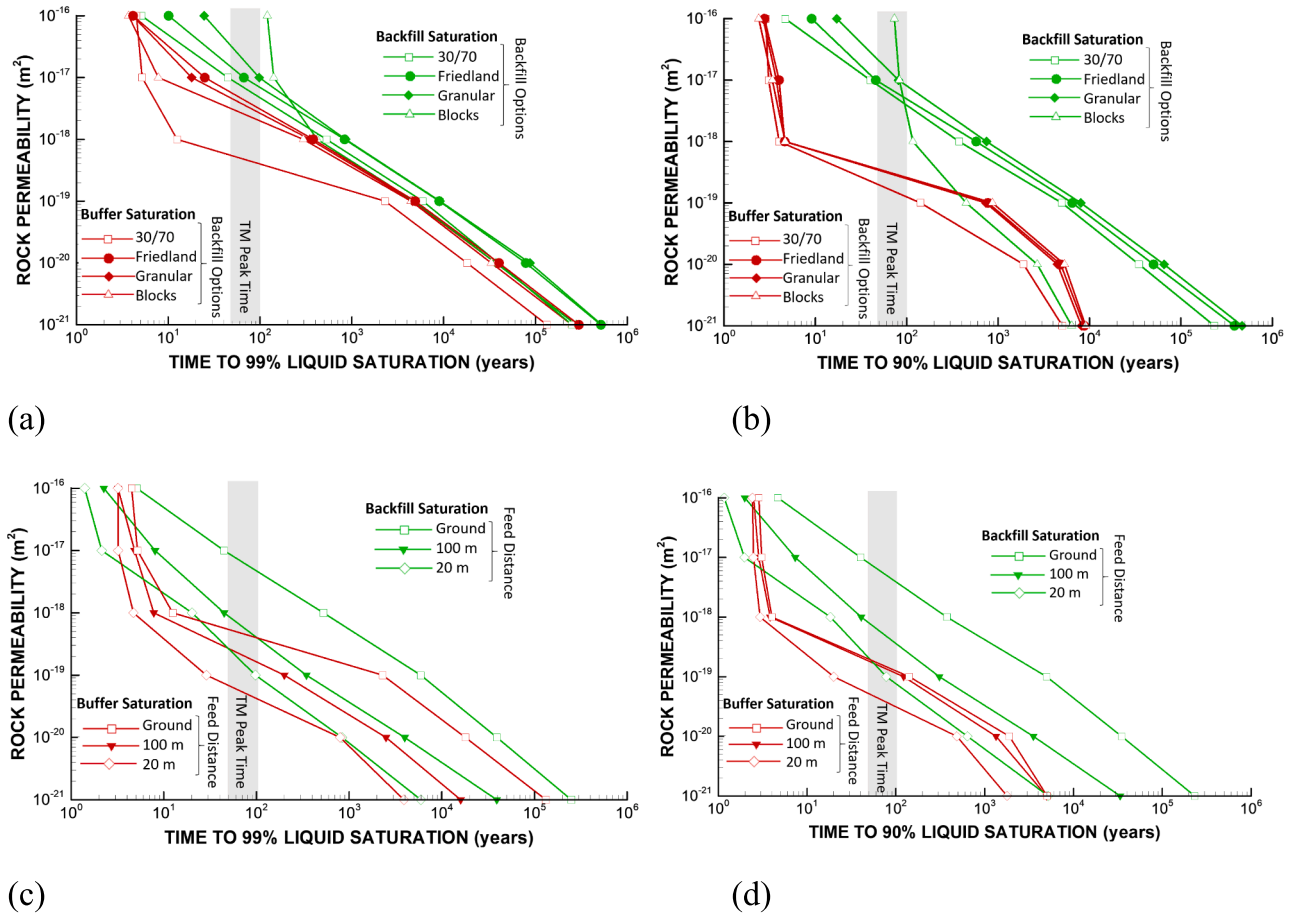

Fig. 15. Results of sensitivity study on buffer and backfill saturation time as function of rock permeability presented as (a) time to 99% saturation for various backfill options, (b) time to 90% saturation for various backfill options, (c) time to 99% saturation for various lengths to a water-feeding boundary, and (d) time to 90% saturation for various lengths to a water-feeding boundary.

evolutions calculated in SKB's and Posiva's thermal management analyses for the Forsmark (Hökmark et al., 2009) and Olkiluoto sites (Pintado Rautioaho, 2012; Ikonen and Raiko, 2012; Toprak et al., 2012), at least until 1000 years. The calculated longer term temperature, i.e. after 10,000 years, in this kind of vertical column model tends to be somewhat overestimated compared to the full 3D repository scale analyses in Hökmark et al., (2009) and Ikonen and Raiko (2012). In terms of thermal evolution, the confidence in temperature prediction until 1000 years is relatively high as well as the prediction of a peak temperature well below 100°C at about 50 years. The peak temperature within the canisters might be slightly higher in case there is gap between the buffer and canister that remains open at the time of the peak temperature (Hökmark et al., 2009; Toprak et al., 2012: Ikonen and Raiko, 2012). If necessary, the waste canister and buffer peak temperature can be lowered by engineering the buffer for high thermal conductivity (Rutqvist, 2020; Lee et al., 2023; Feng et al., 2024). In this study, the main concern is rather the peak temperature in the host rock, which is the driving force for the thermal–mechanical stress and potential rock damage.

6.2. Hydrological evolution and saturation time

In general, the large range of saturation times obtained in this analysis is consistent with results obtained by SKB and Posiva for the Forsmark and Olkiluoto repositories (Posiva, 2021; SKB 2022b). The rock permeability of $1x10^{-19}$ m^2 we estimated as required to achieve 90% saturation before the thermal–mechanical peak, should be compared with estimated of permeability of the two sites. A mean permeability of $1x10^{-19}$ m^2 has been estimated for the Olkiluoto site, though matrix permeability cold be as low as $1x10^{-21}$ m^2 (Vaittinen et al., 2020; Posiva, 2021). At Forsmark, rock permeability outside water bearing fractures may range on the order of $1x10^{-21}$ m^2 to $1x10^{-19}$ m^2 (SKB 2022b; Åkesson et al., 2010; Vilks, 2007). Thus, it appears that the buffer and backfill may in many cases not be 90 % saturated before the thermal–mechanical peak (i.e. before 50 to 100 years).

Our analysis with different backfill options highlights a strong interaction between buffer, backfill and host rock through capillary suction. The analysis shows that the time to full saturation of the buffer and backfill is to a large extent dependent on the saturation evolution of the backfilled tunnel. The backfilled tunnel may take the longest to saturate as a results of a large and dominant total pore volume that needs to be filled up by inflowing water. This also means that all the components, of buffer, backfill and host rock should be included when estimating the time to full saturation. Fig. 16 illustrates the difference in the near field saturation behavior around the time of thermal peak (100 years) for different backfill options. We note that desaturation of the host rock has occurred in all the cases when the buffer or backfill material has higher initial suction than that of the host rock. The red contours in the host rock indicate a saturation less than 10%, which according to Fig. 3b would correspond to a liquid phase flow permeability of $k < 1.0 \times 10^{-24}$ m^2, i.e. practically impermeable to liquid flow. A high capillary suction in the buffer or backfill can offset such low permeability effect by a strong capillary suction gradient for liquid flow. Nevertheless, the results in Fig. 16 and our sensitivity study show that the type of backfill material selection have an impact on the saturation time. A backfill conditioned at relatively low capillary suction can supply water to partially saturate the buffer, while a backfill conditioned

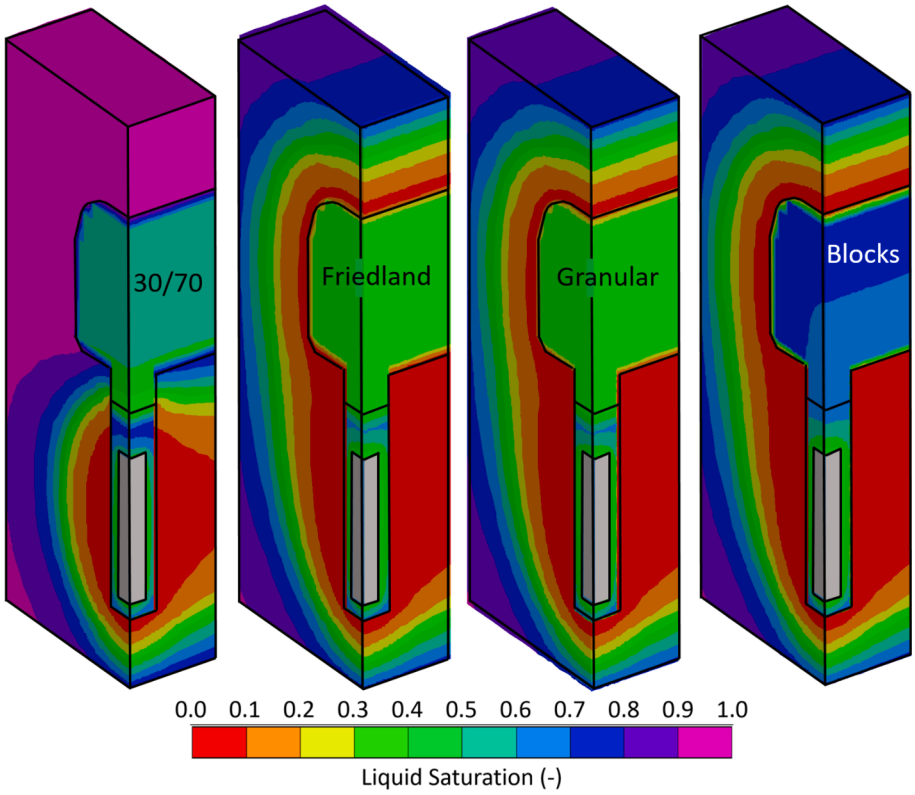

Fig. 16. Contours of the degree of liquid saturation at the thermal–mechanical peak, 100 years after disposal, considering different tunnel backfill options with the hydraulic properties listed in Table 2.

at relatively high suction can help to draw water from the surrounding host rock at a higher rate and thereby accelerate saturation and swelling stress development.

6.3. Mechanical evolution and thermal–mechanical damage to excavations

Our analysis shows that if the saturation is timely, i.e. sufficient saturation occurring before the thermal–mechanical stress peak, widespread damage may not occur around the deposition holes. A tunnel orientation sub-parallel to the maximum horizontal stress, as planned for both the Forsmark and Olkiluoto repositories, is important for minimizing the potential for excavation damage. Our analysis shows that if deposition holes stay dry due to delayed saturation, there is an increased potential for damage around deposition holes, for both the Forsmark and Olkiluoto models. This is for a calculated stress evolution that is essentially consistent with SKB's and Posiva's analyses (Hökmark et al., 2010; Valli et al., 2021). For example Hökmark et al. (2010) calculates a compressive tangential stress of up around 140–150 MPa at the mid-depth of the deposition hole in the Forsmark case, which is consistent with our results. As pointed out by Hökmark et al. (2010), this would exceed the estimated 130 MPa in situ uniaxial compressive strength. Due to the uncertainly whether or not a support pressure will develop, currently the SKB assume conservatively that a spalling zone of high permeability will occur along the deposition holes (Hökmark et al., 2010; SKB, 2022a). In such a case, the extent and permeability of the spalling zone have to be estimated (Martin, 2005; Andersson et al., 2009b).

There would also be an increased potential for stress-induced damage on the top and bottom of the tunnels, but our analysis indicates that this may not occur even if backfill swelling stress does not develop. This is also consistent with the results of Hökmark et al. (2010) for the Forsmark repository case. For the Olkiluoto modeling case, we found that damage in the form of foliation shear could occur at the top and bottom of the tunnels. This is in agreement with 3DEC modeling by Valli et al. (2021) that indicated similar damage zone for the case of no swelling stress. In our analysis, the foliation shear would occur even if backfill swelling occurs with a swelling stress of 3 MPa before the thermal–mechanical peak. It should be clarified, as pointed out in Valli et al., (2021; 2023), that the foliation shear would not be expected to create a continuous zone of enhanced permeability because any damage occurrence would be heterogeneous depending on the local foliation orientation and shear strength. In fact, the foliation shear may help to relieve high compressive stress and thereby prevent brittle spalling failure that could be more detrimental in causing a continuous spalling zone along the deposition holes. Investigations reported in Follin et al. (2021), on excavation induced changes (no thermal stress), also indicates discontinuous fracturing below the tunnel that appears to not form a continuous flow path along the tunnel.

As mentioned, our analysis shows that tensile stress can develop in the sidewalls of the emplacement tunnels. Such tensile stress would develop after emplacement and closure, during the thermal period. The tension in the sidewalls of the emplacement tunnels would tend to open up pre-existing sub-horizontal fractures, or extend such fracture by propagation. This could potentially induce a continuous zone of increased permeability along the tunnels. While current studies have been focused on EDZ due at the excavation stage and changes in the high compressive stress zones such a below and above tunnels (Kwon et al., 2006; Ericsson et al., 2015; Cho et al., 2017; Follin et al., 2021; Valli et al., 2021) the potential for thermal-mechanically-induced tensile fracturing in the tunnel sidewalls does not seem to have been investigated, although indicated in theoretic studies (Nguyen et al., 2009; Hudson et al., 2009; Rutqvist et al., 2009c).

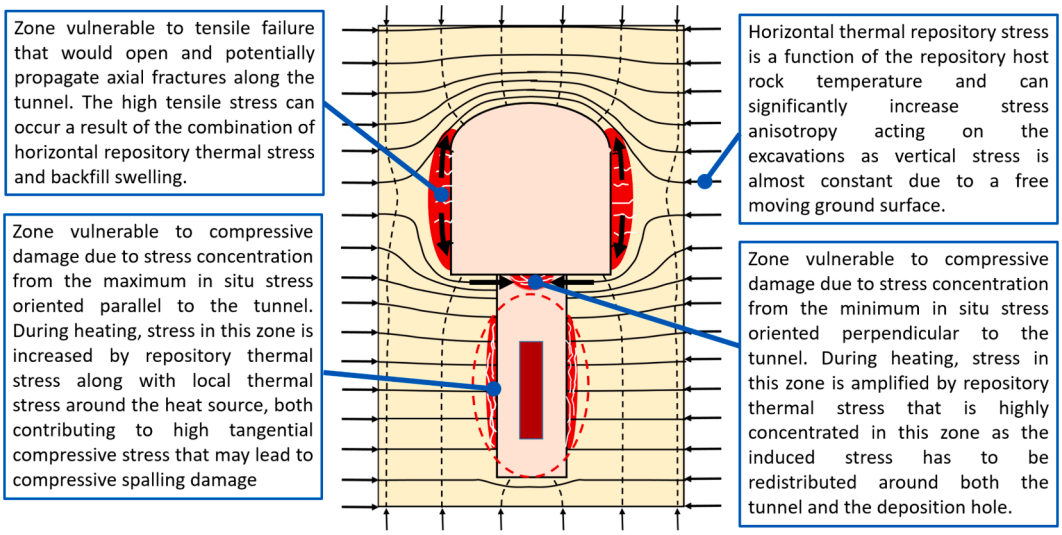

Fig. 17. Schematic of near-field stress trajectories and areas most vulnerable to thermal–mechanical damage for a KBS-3V repository design with emplacement tunnels parallel to the maximum compressive in situ stress.

6.4. Model limitations and uncertainties

The main limitations and uncertainties in this study in terms of the estimation of the damage potential for the Forsmark and Olkiluoto models would be the uncertainties in (1) the initial stress field, (2) the estimated swelling stress evolution in buffer and backfill, (3) the estimated in situ rock strength. In terms of the initial stress field, the maximum compressive stress might be the most uncertain and could have an impact on the potential for damage on the deposition hole. Estimates at both sites show considerable variation in the measured values (Figuiredo et al., 2022; Mattila et al., 2022). Related to the buffer swelling stress evolution, it should be acknowledged that the linear swelling model applied in this analysis would likely tend to overestimate the swelling stress at partial saturation, i.e. before full saturation (Rutqvist et al., 2011). For bentonite, most of the swelling and swelling stress development occurs at high saturation. Such non-linear swelling can be considered for a more accurate stress path using more advance unsaturated soil mechanics models (e.g. Rutqvist et al., 2011; Rutqvist, 2015), though these models will require more input parameters that may not be readily available for all buffer and backfill options.

Connected to this are also model limitations and uncertainties related to the hydraulic saturation of the buffer. There are significant uncertainties in the water retention and relative permeability curves for the host rock. We applied water retention and relative permeability curves back-calculated from a crystalline rock site having a rock permeability of 1×10^{-18} m^2, which correspond to an average of the low- and high-permeability values considered in this study. Thus, these curves are realistic for crystalline rock, but more investigations are needed to understand their variations, such as in fractures and rock matrix. Moreover, delayed saturation due to micro–macro-structural bentonite interactions may also play a role (Thomas et al., 2003; Sanchez et al., 2012; Vilarrasa et al., 2016). On the other hand, such micro–macro-scale interactions would also occur in the laboratory infiltration experiments used to calibrate the current relative permeability model and would therefore be intrinsically accounted for in the current analysis.

Finally, the in situ rock strength is still uncertain, perhaps more so for the Forsmark site as no in situ spalling experiments has been conducted there yet. In particular, the impact of confining stress from a buffer and backfill would need further investigations and field tests at both Forsmark and Olkiluoto. Previous experiments at the Äspö Hard Rock Laboratory investigating the impact of applied confinement to prevent spalling were inconclusive (Glamheden et al., 2010). Such in situ tests including confining stress effects could provide inputs for more detailed models regarding the in situ strength, considering cohesion loss and friction mobilization. This would also allow for elasto-plastic modeling of the rock damage, such a continuum damage models (Souley et al., 2001; Nguyen, 2021) compared to the simplified stress analysis performed in this study. Still, such analysis would be limited to continuum mechanics, while more complex discontinuous models (Lisjak and Grasselli, 2014; Farahmand and Diederichs, 2021; Hu and Rutqvist, 2022; Saceanu et al., 2022; Shen et al., 2024) may be applied to explicitly represents grains and fractures, and resulting permeability change to the damage zone. However, any complex numerical methods and model conceptualization will be associated with additional model and data uncertainties. Due to the heterogeneous nature of the rock and detailed information required for such analysis, predicting damage at the repository-scale may require a statistical approach (e.g. Martin and Christiansson, 2009; Siren et al., 2015), which is out of the scope of this study.

7. Concluding remarks

We conducted coupled thermo-hydro-mechanical (THM) modeling associated with KBS-3V nuclear waste disposal in crystalline rocks, using data and conditions from the Forsmark and Olkiluoto repository sites in Sweden and Finland. The study addresses repository performance around thermal and hydraulic evolutions, and their impact on the potential for thermal–mechanical damage to the underground repository excavations. Damage to excavation walls can impact the repository safety by creating permeable zones along deposition holes and along tunnels that could impact radionuclide transport properties.

The analyses using the Forsmark and Olkiluoto models show that local hydraulic rock properties, including permeability and water retention of the buffer, backfill and the host rock has a strong impact on THM evolution and the potential for inducing thermal–mechanical damage to the repository excavations. The analysis shows that depending on the distance to a water-feeding boundary, a 90 % saturation of the buffer can be achieved before the thermal–mechanical peak at 50–100 years if the permeability is on the order of $1x10^{-19}$ m^2 or higher. Because permeability at Forsmark and Olkiluoto is estimated to locally be lower than $1x10^{-19}$ m^2 there is a high potential for developing thermal–mechanical damage around deposition holes. At the Forsmark site, this could result in a brittle spalling zone of enhanced permeability along the deposition holes. At the Olkiluoto site, this would more likely be thermal-mechanically induced foliation shear that due to its

heterogeneous nature may not create a continuous permeable damage zone.

Our analysis indicates much less potential for compressive damage on top and bottom of the tunnels, except for foliation shear that could occur at the Olkiluoto site. On the other hand, the analysis using both the Forsmark and Olkiluoto models, show a high potential for tensile stress and failure in the sidewalls of the tunnels. This may be significant because such tensile stress could open up existing fractures, that could propagate, forming a continuous damaged zone along the tunnels, i.e. providing a flow path for radionuclide transport.

Based on our results for the two repository site models, we make a few general remarks regarding prediction of thermal–mechanical damage of a KBS-3V nuclear waste repository in crystalline host rocks with reference to Fig. 17:

- The deposition holes are most vulnerable to compressive thermal–mechanical damage, in particular if buffer saturation and swelling is not sufficient before the thermal–mechanical peak.
- The sidewalls of emplacement tunnels may be vulnerable to tensile failure and creation of an axial flow path due to combined thermal stressing and backfill swelling.
- If, where and when thermal–mechanical damage can be induced very much depends on the local stress field which should be evaluated as precisely as possible, including maximum and minimum horizontal stress magnitudes.
- Site specific in situ experiments are instrumental for identifying failure modes and constraining in situ rock wall strength, that could vary significantly from site to site.
- A careful analysis and design of the repository layout and the backfill/buffer material selection can help to minimize the potential for thermal–mechanical damage of repository excavations.

In general, this analysis highlights the strong interactions between the relevant components of backfill, buffer and host rock, meaning that all these components have to be included when predicting the long-term coupled THM processes and when evaluating the potential for thermal–mechanical damage that may occur hundreds of years after waste deposition and closure of the repository.

CRediT authorship contribution statement

J. Rutqvist: Writing – review & editing, Writing – original draft, Visualization, Software, Methodology, Investigation, Funding acquisition, Formal analysis, Conceptualization. **C.-F. Tsang:** Writing – review & editing, Supervision, Methodology, Funding acquisition, Conceptualization.

Declaration of competing interest

The authors declare that they have no known competing financial interests or personal relationships that could have appeared to influence the work reported in this paper.

Data availability

Data will be made available on request.

Acknowledgments

This work was funded in part by grants from the Swedish Radiation Safety Authority (SSM) and Finish Radiation and Nuclear Safety Authority (STUK) through the U.S. Department of Energy (DOE) Contract no. DE-AC02-05CH11231 with Lawrence Berkeley National Laboratory. The statements made in the paper are, however, solely those of the authors and do not necessarily reflect those of the funding agencies. The authors would like to thank the two anonymous reviewers for valuable comments that improved the quality of the paper.

References

Ahn, J., Apted, M.J., 2010. Geological Repository Systems for Safe Disposal of Spent Nuclear Fuels and Radioactive Waste, 1st ed. Elsevier, pp. 792.

Åkesson, M., Kristensson, O., Börgesson, L., Dueck, A., Hernelind, J., 2010. THM modelling of buffer, backfill and other system components - Critical processes and scenarios. SKB Technical Report TR-10-11. Swedish Nuclear Fuel and Waste Management Co, Stockholm, Sweden. March 2010.

Alonso, E.E., Alcoverro, J., Coste, F., Malinsky, L., Merrien Soukatchoff, V., Kadiri, I., Nowak, T., Shao, H., Nguyen, T.S., Selvadurai, A.P.S., Armand, G., Sobolik, S.R., Itamura, C.M., Stone, C.M., Webb, S.W., Rejeb, A., Tijani, M., Maouche, Z., Kobayashi, A., Kurikami, H., Ito, A., Sugita, Y., Chijimatsu, M., Börgesson, L., Hernelind, J., Rutqvist, J., Tsang, C.F., Jussila, P., 2005. The FEBEX Benchmark test. Case Definition and comparison of modelling approaches. Int. J. Rock Mech. Min. Sci. 42, 611–638.

Andersson, J.C., Martin, C.D., 2009a. The Äspö pillar stability experiment: Part I—Experiment design. Int. J. Rock Mech. Min. Sci. 46, 865–878.

Andersson, J.C., Martin, C.D., Stille, H., 2009b. The Äspö pillar stability experiment: Part II—Rock mass response to coupled excavation-induced and thermal-induced stresses. Int. J. Rock Mech. Min. Sci. 46, 879–895.

Autio, J., Hassan, Md. M., Karttunen, P., Keto, P., 2012. Backfill design 2012. Posiva report 2012-15. Posiva OY, Eurajoki. Finland.

Biot, M.A., 1941. General theory of three dimensional consolidation. J. Appl. Phys. 12, 155–164.

Birkholzer, J.T., Tsang, C.F., Bond, A.E., Hudson, J.A., Jing, L., Stephansson, O., 2019. 25 years of DECOVALEX - scientific advances and lessons learned from an international research collaboration in coupled subsurface processes. Int. J. Rock Mech. Min. Sci. 122, 103995.

Börgesson, L. Hernelind, J., 1999. Coupled thermo-hydro-mechanical calculations of the water saturation phase of a KBS-3 deposition hole. Influence of hydraulic rock properties on the water saturation phase. SKB TR-99-41. Swedish Nuclear Fuel and Waste Management Co, Stockholm, Sweden.

Börgesson, L, Gunnarsson, D., Johannesson, L.-E., Sandén, T., 2002. Äspö Hard Rock Laboratory. Prototype Repository. Installation of buffer, canisters, backfill and instruments in Section 1. SKB IPR-02-23. Swedish Nuclear Fuel and Waste Management Co, Stockholm, Sweden.

Börgesson, L., Fälth, B., Hernelind, J., 2006. Water saturation phase of the buffer and backfill in the KBS-3V concept. Special emphasis given to the influence of the backfill on the wetting of the buffer. SKB TR-06-14. Swedish Nuclear Fuel and Waste Management Co, Stockholm, Sweden.

Börgesson, L., Dixon, D., Gunnarsson, D., Hansen, J., Jonsson, E., Keto, P., 2009. Assessment of backfill design for KBS-3V repository. Posiva Working report 2009-115.Posiva OY, Eurajoki. Finland.

Chijimatsu, M., Nguyen, T.S., Jing, L., De Jonge, J., Kohlmeier, M., Millard, A., Rejeb, A., Rutqvist, J., Souley, M., Sugita, Y., 2005. Numerical study of the THM effects on the near-field safety of a hypothetical nuclear waste repository – BMT1 of the DECOVALEX III project. Part 1: Conceptualization and characterization of the problems and summary of results. Int. J. Rock Mech. Min. Sci. 42, 720–730.

Chijimatsu, M., Börgesson, L., Fujita, T., Jussila, P., Nguyen, S., Rutqvist, J., Jing, L., 2009. Model development and calibration for the coupled thermal, hydraulic and mechanical phenomena of the bentonite. Environ. Geol. 57, 1255–1261.

Cho, W.J., Lee, C., Kim, G.Y., 2017. Feasibility analysis of the multilayer and multicanister concepts for a geological spent fuel repository. Nucl. Technol. 200, 225–240.

Cleall, P.J., Melhuish, T.A., Thomas, H.R., 2006. Modeling the three-dimensional behaviour of a prototype nuclear waste repository. Eng. Geol. 85 (1–2), 212–229.

Dueck, A., Nilsson, U., 2010. Thermo-Hydro-Mechanical properties of MX-80. Results from advanced laboratory tests. SKB TR-10-55. Swedish Nuclear Fuel and Waste Management Co, Stockholm, Sweden.

Ericsson, L.O., Thörn, J., Christiansson, R., Lehtimäki, T., Ittner, H., Hansson, K., Butron, C., Sigurdsson, O., Kinnbom, P., 2015. A demonstration project on controlling and verifying the excavation-damaged zone. SKB R-14-30. Swedish Nuclear Fuel and Waste Management Co, Stockholm, Sweden.

Farahmand, K., Diederichs, M.S., 2021. Calibration of coupled hydro-mechanical properties of grain-based model for simulating fracture process and associated pore pressure evolution in excavation damage zone around deep tunnels. J. Rock Mech. Geotech. Eng. 13, 60–83.

Faybishenko, B., Birkholzer, J., Sassani, D., Swift P., 2016. International Approaches for Deep Geological Disposal of Nuclear Waste: Geological Challenges in Radioactive Waste Isolation: Fifth Worldwide Review. Lawrence Berkeley National Laboratory Report, LBNL-1006984. https://eesa.lbl.gov/wwr5/. Berkeley, California.

Feng, Y., Eun, J., Kim, S., Kim, Y.R., 2024. Evaluation of equivalent thermal conductivity for carbon fiber-reinforced bentonite through experimental and numerical analysis. Comput. Geotech. 165, 105880.

Figuiredo, B., Mattila, J., Sjöberg, J., Hakala, M., 2022. Analysis and determination of the stress field at the Olkiluoto site. Posiva Working report 2009-115. Posiva OY, Eurajoki. Finland. May 2022.

Finsterle, S., Pruess, K., 1995. Solving the estimation-identification problem in two-phase flow modeling. Water Resour. Res. 31, 913–924.

Follin, S., Koskinen L., Suikkanen J., Riihiluoma N., Kantia P., Kiuru R., Mustonen S. 2021. Characterization of EDZ for Final Disposal Facility of Spent Nuclear Fuel in Olkiluoto. POSIVA 2021-16. Posiva Oy, Eurajoki, Finland.

Freundlich, H., 1909. Kapillarchemie: Eine Darstellung der Chemie der Kolloide und verwandter Gebiete [Capillary Chemistry: A presentation of colloid chemistry and related fields] (Leipzig, Germany: Akademische Verlagsgesellschaft).
Geier, J., Bath, A., Stephansson, O., 2012. Comparison of site descriptive models for Olkiluoto, Finland and Forsmark, Sweden. STUK-TR 14. Radiation and Nuclear Safety Authority, Helsinki, Finland.
Gens, A, Sanchez. M, Guimaraes. L,D,N, Alonso, E., Lloret, A., Olivella, S. et al., 2009. A full-scale in situ heating test for high-level nuclear waste disposal: observations, analysis and interpretation. Geotech., 59(4), 377-99.
Glamheden, R., Fredriksson, A., Röshoff, K., Karlsson, J., Hakami, H., Christiansson, R., 2007. Rock mechanics Forsmark. Site descriptive modelling Forsmark stage 2.2. SKB R-07-31. Swedish Nuclear Fuel and Waste Management Co, Stockholm, Sweden.
Glamheden, R., Fälth, B., Jacobsson, L., Harrström, J., Berglund, J.., Bergkvist, L., 2010. Counterforce applied to prevent spalling. SKB TR-10-37. Swedish Nuclear Fuel and Waste Management Co, Stockholm, Sweden.
Hakala, M., Valli, J., Juvani, J., 2018. ONKALO POSE Experiment - 3DEC Back Analyses. Working Report 2018-15. Posiva OY, Eurajoki. Finland.
Hedin, A., Olsson, O., 2016. Crystalline rock as a repository for Swedish spent nuclear fuel. ELEMENTS, VOL. 12, PP. 247–252. August 2016.
Hökmark, H., Lönnqvist, M., Kristensson, O., Sundberg, J., Hellström, G., 2009. Strategy for thermal dimensioning of the final repository for spent nuclear fuel. SKB R-09-04. Swedish Nuclear Fuel and Waste Management Co, Stockholm, Sweden.
Hökmark, H., Lönnqvist, M., Fälth, B., 2010. THM-issues in repository rock - Thermal, mechanical, thermo-mechanical and hydro-mechanical evolution of the rock at the Forsmark and Laxemar sites. SKB TR-10-23. Swedish Nuclear Fuel and Waste Management Co, Stockholm, Sweden.
Hu, M., Rutqvist, J., 2022. Multi-scale coupled processes modeling of fractures as porous, interfacial and granular systems from rock images with the numerical manifold method. Rock Mech. Rock Eng. 55, 3041–3059.
Hudson, J.A., Bäckström, A., Rutqvist, J., Jing, L., Backers, T., Chijimatsu, M., Christiansson, R., Feng, X.-T., Kobayashi, A., Koyama, T., Lee, H.-S., Neretnieks, I., Pan, P.-Z., Rinne, M., Shen, B., 2009. Characterising and modelling the excavation damaged zone (EDZ) in crystalline rock in the context of radioactive waste disposal. Environ. Geol. 57, 1275–1297.
Ikonen, K., Raiko, H., 2012. Thermal dimensioning of Olkiluoto repository for spend fuel. Working Report POSIVA 2012-56. Posiva Oy, Olkiluoto.
Ikonen, K., Kuutti, J., Raiko, H., 2018. Thermal dimensioning for the Olkiluoto Repository — 2018 Update. Posiva Working Report 2018-26. Posiva Oy, Olkiluoto.
Jaeger, J.C., Cook, N.G.W., Zimmerman, R.W., 2007. Fundamentals of rock mechanics. New York, USA: Wiley-Blackwell; 2007.
Johannesson, L.E., Nilsson, U., 2006. Deep repository – engineered barrier systems: Geotechnical behaviour of candidate backfill materials - Laboratory tests and calculations for determining performance of the backfill. SKB R-06-73. Swedish Nuclear Fuel and Waste Management Co, Stockholm, Sweden.
Kim, K.I., Lee, C., Cho, D., Rutqvist, J. 2024. Enhancement of disposal efficiency for deep geological repositories based on three design factors - Decay heat optimization, increased thermal limit of the buffer and double-layer concept. Tunnelling and Underground Space Technology (in revision).
Kwon, S., Choi, J.W., 2006. Thermo-mechanical stability analysis for a multi-level radioactive waste disposal concept. Geotech. Geol. Eng. 24, 361–377.
Lee, C., Lee, J., Park, S., Kwon, S., Cho, W.J., Kim, G.Y., 2020. Numerical analysis of coupled thermo-hydro-mechanical behavior in single and multi-layer repository concepts for high-level radioactive waste disposal. Tunn. Undergr. Space Technol. 103 (1–17), 103452.
Lee, G.J., Yoon, S., Kim, T., Chang, S., 2023. Investigation of the various properties of several candidate additives as buffer materials. Nucl. Eng. Technol. 55, 1191–1198.
Lisjak, A., Grasselli, G., 2014. A review of discrete modeling techniques for fracturing processes in discontinuous rock masses. J. Rock Mech. Geotech. Eng. 6, 301–314.
Martin, C.D., 1997. The effect of cohesionloss and stress path on brittle rock strength. Can. Geotech. J. 34, 698–725.
Martin, C.D., Christiansson, R., 2009. Estimating the potential spalling around a deep nuclear waste repository in crystalline rock. Int. J. Rock Mech. Min. Sci. 46, 219–228.
Martin, C.D., Read, R.S., Martino, J.B., 1997. Observations of brittle failure around a circular test tunnel. Int. J. Rock Mech. Min. Sci. 34, 1065–1073.
Martin, C.D., 2005. Preliminary assessment of potential underground stability (wedge and spalling) at Forsmark, Simpevarp and Laxemar sites. SKB report R-05-71. Swedish Nuclear Fuel and Waste Management Co, Stockholm, Sweden.
Martino, J.B., Chandler, N.A., 2004. Excavation-induced studies at the underground research laboratory. Int. J. Rock Mech. Min. Sci. 41, 1413–1426.
Mattila, J., Suikkanen, J., Read, R., Valli, J., Hakala, M., Sjöberg, J., Figueiredo, B., Kiuru, R., Haapalehto, S., 2022. Rock mechanics of Olkiluoto. Povisva 2021-18. Posiva Oy, Eurajoki, Finland.
Millard, A., Rejeb, A., Chijimatsu, M., Jing, L., De Jonge, J., Kohlmeier, M., Nguyen, T.S., Rutqvist, J., Souley, M., Sugita, Y., 2005. Numerical study of the THM effects on the near-field safety of a hypothetical nuclear waste repository – BMT1 of the DECOVALEX III project. Part 2: Effects of THM coupling in continuous and homogeneous rock. Int. J. Rock Mech. Min. Sci. 42, 731–744.
Min, K.B., Lee, J., Stephansson, O., 2013. Implications of thermally-induced fracture slip and permeability change on the long-term performance of a deep geological repository. Int. J. Rock Mech. Min. Sci. 61, 275–288.
Mualem, Y., 1976. A new model for predicting the hydraulic conductivity of unsaturated porous media. Water Resour. Res. 12 (3), 513–522.
Nguyen, T.S., 2021. Progressive damage of a Canadian granite in laboratory compression tests and underground excavations. Minerals 11, 10.
Nguyen, T.S., Börgesson, L., Chijimatsu, M., Rutqvist, J., Fujita, T., Hernelin, J., Kobayashi, A., Onishi, Y., Tanaka, M., Jing, L., 2001. Hydro-mechanical response of a fractured rock mass to excavation of a test pit – The Kamaishi Mine Experiment in Japan. Int. J. Rock Mech. Min. Sci. 38, 79–94.
Nguyen, T.S., Börgesson, L., Chijimatsu, M., Hernelind, J., Jing, L., Kobayashi, A., Rutqvist, J., 2009. A case study on the influence of THM coupling on the near field safety of a spent fuel repository in sparsely fractured granite. Environ. Geol. 57, 1239–1254.
Noorishad, J., Tsang, C.-F., 1996. Coupled thermohydroelasticity phenomena in variable saturated fractured porous rocks—formulation and numerical solution. In: Stephansson O, Jing L, Tsang C-F (eds) Coupled thermo-hydro-mechanical processes of fractured media. Developments in geotechnical engineering, vol 79. Elsevier, Amsterdam, pp 93–134.
NWTRB, 2022. Survey of National Programs for Managing High-Level Radioactive Waste and Spent Nuclear Fuel: 2022 Update. A Report to Congress and the Secretary of Energy. Nuclear Waste Technical Review Board. July 2022.
Philip, J.R., de Vries, D.A., 1957. Moisture movement in porous material under temperature gradients. EOS Trans. AGU 38, 222–232.
Pintado, X., Rautioaho, E., 2012. Thermo-hydraulic modelling of buffer and backfill. Posiva 2012-48. Posiva OY, Eurajoki. Finland.
Posiva, 2003. ONKALO underground characterization and research programme (UCRP). POSIVA 2003-03. Posiva OY, Eurajoki. Finland.
Posiva, 2012a. Safety Case for the Disposal of Spent Nuclear Fuel at Olkiluoto. - Design Basis 2012. Posiva 2012-03. Posiva Oy, Eurajoki.
Posiva, 2012b. Safety Case for the Disposal of Spent Nuclear Fuel at Olkiluoto -Description of the Disposal System 2012. POSIVA 2012-05. Posiva Oy, Eurajoki, Finland.
Posiva, 2021. Buffer, backfill and closure evolution. POSIVA 2021-08. Posiva Oy, Eurajoki, Finland, December 2021.
Posiva-SKB, 2017. Safety functions, performance targets and technical design requirements for a KBS-3V repository. Posiva SKB Report 02, January 2017. Posiva OY, Eurajoki. Finland.
Richards, L.A., 1931. Capillary conduction of liquids through porous mediums. Physics 1, 318–333.
Rutqvist, J., 2020. Thermal management associated with geologic disposal of large spent nuclear fuel canisters in tunnels with thermally engineered backfill. Tunn. Undergr. Space Technol. 102, 103454.
Rutqvist, J., Tsang, C.-F., 2008. Review of SKB's Work on Coupled THM Processes Within SR-Can: External review contribution in support of SKI's and SSI's review of SR-Can. Swedish Nuclear Power Inspectorate (SKI) Technical Report 2008:08.
Rutqvist, J., Barr, D., Birkholzer, J.T., Fujisaki, K., Kolditz, O., Liu, Q.-S., Fujita, T., Wang, W., Zhang, C.-Y., 2009a. A comparative simulation study of coupled THM processes and their effect on fractured rock permeability around nuclear waste repositories. Environ. Geol. 57, 1347–1360.
Rutqvist, J., Börgesson, L., Chijimatsu, M., Hernelind, J., Jing, L., Kobayashi, A., Nguyen, S., 2009b. Modeling of damage, permeability changes and pressure responses during excavation of the TSX tunnel in granitic rock at URL, Canada. Environ. Geol. 57, 1263–1274.
Rutqvist, J., Bäckström, A., Chijimatsu, M., Feng, X.-T., Pan, P.-Z., Hudson, J., Jing, L., Kobayashi, A., Koyama, T., Lee, H.-S., Huang, X.-H., Rinne, M., Shen, B., 2009c. Multiple-code simulation study of the long-term EDZ evolution of geological nuclear waste repositories. Environ. Geol. 57, 1313–1324.
Rutqvist, J., Ijiri, Y., Yamamoto, H., 2011. Implementation of the Barcelona Basic Model into TOUGH-FLAC for simulations of the geomechanical behavior of unsaturated soils. Comput. Geosci. 37, 751–762.
Rutqvist, J., Tsang, C.-F., 2012. Multiphysics processes in partially saturated fractured rock: Experiments and models from Yucca Mountain. Rev. Geophys. 50, RG3006.
Rutqvist, J., Börgesson, L., Chijimatsu, M., Kobayashi, A., Nguyen, T.S., Jing, L., Noorishad, J., Tsang, C.-F., 2001a. Thermohydromechanics of partially saturated geological media – Governing equations and formulation of four finite element models. Int. J. Rock Mech. Mining Sci. 38, 105–127.
Rutqvist, J., Börgesson, L., Chijimatsu, M., Nguyen, T.S., Jing, L., Noorishad, J., Tsang, C.-F., 2001b. Coupled thermo-hydro-mechanical analysis of a heater test in fractured rock and bentonite at Kamaishi Mine – Comparison of field results to predictions of four finite element codes. Int. J. Rock Mech. Min. Sci. 38, 129–142.
Rutqvist, J., Chijimatsu, M., Jing, L., De Jonge, J., Kohlmeier, M., Millard, A., Nguyen, T. S., Rejeb, A., Souley, M., Sugita, Y., Tsang, C.F., 2005. Numerical study of the THM effects on the near-field safety of a hypothetical nuclear waste repository – BMT1 of the DECOVALEX III project. Part 3: Effects of THM coupling in fractured rock. Int. J. Rock Mech. Min. Sci. 42, 745–755.
Rutqvist, J., Barr, D., Birkholzer, J.T., Chijimatsu, M., Kolditz, O., Liu, Q.-S., Oda, Y., Wang, W.-Q., Zhang, C.-Y., 2008. Results from an international simulation study on coupled thermal, hydrological, and mechanical (THM) processes near geological nuclear waste repositories. Nucl. Technol. 163, 101–109.
Rutqvist, J., 2015. Coupled Thermo-Hydro-Mechanical Behavior of Natural and Engineered Clay Barriers. In Tournassat, Steefel, Bourg and Bergaya editors. Natural and Engineered Clay Barriers. Elsevier. pp. 329-255.
Saceanu, M.C., Paluszny, A., Zimmerman, R.W., Mas Ivars, D., 2022. Fracture growth leading to mechanical spalling around deposition boreholes of an underground nuclear waste repository. Int. J. Rock Mech. Min. Sci. 152, 105038.
Sánchez, M., Gens, A., Olivella, S., 2012. THM analysis of a largescale heating test incorporating material fabric changes. Int. J. Numer. Anal. Methods Geomech. 36 (4), 391–421.
Sedeer, E.S., 2022. Final resting place - Finland is set to open the world's first permanent repository for high-level nuclear waste. How did it succeed when other countries stumbled? 25 FEBRUARY 2022 SCIENCE science.org • VOL 375 ISSUE 6583.

Seo, E., Kim, K.-I., Yoo, H., Yoon, J., Min, K.-B., 2024. Far-field analysis of shear slip potential and ground uplift by high-level radioactive waste repositories with single- and multi-canister and multi-layer disposal concepts. Tunn. Undergr. Space Technol. 145, 105611.

Shen, B., Khanal, M., Shi, J., Mallants, D., 2024. Modelling geomechanical stability of a large deep borehole in shale for radioactive waste disposal. Tunn. Undergr. Space Technol. 145, 105606.

Siren, T., 2017. Overview of Finnish spent nuclear fuel disposal programme. J. Korean Soc. Miner. Energy Resour. Eng. 54 (4), 367–376.

Siren, T., Hakala, M., Valli, J., Kantia, P., Hudson, J.A., Johansson, E., 2015. In situ strength and failure mechanisms of migmatitic gneiss and pegmatitic granite at the nuclear waste disposal site in Olkiluoto, Western Finland. Int. J. Rock Mech. Mining Sci. 79, 135–148.

SKB, 2006. Long-term safety for KBS-3 repository at Forsmark and Laxemar – a first evaluation. Main report of the SR-Can project. SKB TR-06-09. Swedish Nuclear Fuel and Waste Management Co, Stockholm, Sweden.

SKB, 2008. Site description of Forsmark at completion of the site investigation phase. Technical Report TR-08-05, Swedish Nuclear Fuel and Waste Management Co., Stockholm, Sweden.

SKB, 2022a. Post-closure safety for the final repository for spent nuclear fuel at Forsmark Main report, PSAR version. SKB Technical Report TR-21-01. Swedish Nuclear Fuel and Waste Management Co, Stockholm, Sweden. December 2022.

SKB, 2022b. Post-closure safety for the final repository for spent nuclear fuel at Forsmark. Model summary report, PSAR version. SKB Technical Report TR-21-05. Swedish Nuclear Fuel and Waste Management Co, Stockholm, Sweden. December 2022.

SKB, 2022c. Post-closure safety for the final repository for spent nuclear fuel at Forsmark Data report, PSAR version. SKB Technical Report TR-21-06. Swedish Nuclear Fuel and Waste Management Co, Stockholm, Sweden. December 2022.

SKB, 2022d. Post-closure safety for the final repository for spent nuclear fuel at Forsmark Buffer, backfilland closure process report, PSAR version. SKB Technical Report TR-21-03. Swedish Nuclear Fuel and Waste Management Co, Stockholm, Sweden. December 2022.

SKBF/KBS, 1983. Final Storage of Spent Nuclear Fuel – KBS-3. Parts I-IV. Swedish Nuclear Fuel Supply Co (KBS Division of SKBF), Stockholm, 574 pp.

Souley, M., Homand, F., Pepa, S., Hoxha, D., 2001. Damage-induced permeability changes in granite: A case example at the URL in Canada. Int. J. Rock Mech. Min. Sci. 38, 297–310.

Suikkanen, J., Lönnqvist, M, Hökmark, H., 2016. Analyses of the stability of a KBS-3H deposition drift at the Olkiluoto Site during Excavation, Thermal loading and Glacial Loading. Posiva 2016-15.

Thomas, H.R., Cleall, P.J., Chandler, N., Dixon, D., Mitchell, H.P., 2003. Water infiltration into a large-scale in-situ experiment in an underground research laboratory. Geotechnique 53 (2), 207–224.

Toprak, E., Mokni, N., Olivella, S., Pintado, X., 2012. Thermo-Hydro-Mechanical Modelling of Buffer Synthesis Report-POSIVA 2012-47. Posiva Oy, Eurajoki, Finland.

Tsang, C.-F. 1987. Coupled processes associated with nuclear waste repositories. Academic Press, Orlando.

Tyler, L. D. (1980), Thermal/mechanical modeling for a tuff repository, in Proceedings of Workshop on Thermalmechanicalhydrochemical Modeling for a Hardrock Waste Repository, Berkeley, California, July 29 to 31, Rep. LBL-11204, pp. 62–69, Lawrence Berkeley Natl. Lab., Berkeley, Calif.

Vaittinen, T., Ahokas, H., Nummela, J., Pentti E., Paulamäki, S., 2020. Hydrogeological structure model of the Olkiluoto Site in 2015. Posiva Working Report 2019-06. Posiva Oy, Eurajoki, Finland.

Valli, J., Mattila, J., Suikkanen, J., Lönnqvist, M., 2021. Rock Mechanics Performance Assessment of KBS-3V Repository at Olkiluoto. Posiva Working Report 2021-25. Posiva Oy, Eurajoki, Finland.

Valli, J., Hakala, M., Mattila, J., Ström, J., Read, R., Siren, T., Suikkanen, J., 2023. Posiva Olkiluoto Spalling Experiment (POSE) Final Report. POSIVA 2023-01. Posiva Oy, Eurajoki, Finland.

van Genuchten, M.T., 1980. A closed-form equation for predicting the hydraulic conductivity of unsaturated soils. Soil Sci. Soc. Am. J. 44, 892–898.

Vilarrasa, V., Rutqvist, J., Blanco-Martin, L., Birkholzer, J., 2016. Use of a dual structure constitutive model for predicting the long-term behavior of an expansive clay buffer in a nuclear waste repository. ASCE's International Journal of Geomechanics, 16, article number D4015005.

Vilks, P., 2007. Forsmark site investigation. Rock matrix permeability measurements on core samples from borehole KFM01D. SKB P-07-162, Svensk Kärnbränslehantering AB.

Vira, J., 2006. Further Steps Towards Licensing: Underground Characterisation Started for the Spent Fuel Repository in Finland. MRS Online Proceedings Library 932, 1241. https://doi.org/10.1557/PROC-932-124.1.

Wang, W., Rutqvist, J., Görke, U.-J., Birkholzer, J.T., Kolditz, O., 2011. Non isothermal flow in low permeable porous media: A comparison of Richards' and two-phase flow approaches. Environ. Earth Sci. 62, 1197–1207.

Zou, L., Cvetkovic, V., 2023. Disposal of high-level radioactive waste in crystalline rock: On coupled processes and site development. Rock Mech. Bull. 2, 100061.